# FINAL REPORT

Contract NASw-1398

# ROCKET STUDY OF X-RAYS FROM THE NON-FLARING SUN

27 September 1969


Loren W. Acton

Palo Alto Research Laboratories

Lockheed Missiles & Space Company

Palo Alto, California

## ABSTRACT

A series of 3 rocket flights have been carried out for the purpose of measuring the high-energy tail of the x-ray spectrum of the quiescent sun. This emission has been shown to be highly variable in intensity and slope but with spectral distributions which may be adequately described in terms of thermal bremsstrahlung.

Incidental to the solar measurements data were obtained on several discrete cosmic x-ray sources and the diffuse cosmic x-ray background. The time-integrated x-ray emission of the crab nebula and the diffuse cosmic emission can both be described in terms of power law spectra with intensity and slope in essential agreement with the results of other workers.

## Table of Contents

B. "Observations of Energetic X-Rays from Quiescent Solar Active Regions," Acton, L. W., and Fisher, P. C., in Structure and Development of Solar Active Regions, ed. K. O. Kiepenheuer, p. 432, (D. Reidel Publ. Co., Dordrecht, 1968).

C. "Spectrum of the Crab X-Ray Source from 4 to 40 keV," Acton, L. W., Catura, R. C., and Fisher, P. C., Bul. Am. Astron. Soc., (1969). Abstract of paper presented at 129th meeting of the American Astronomical Society, Honolulu, Hawaii.

# I. INTRODUCTION

The objective of the experiments carried out under Contract NASw-1398 was to obtain a series of measurements of the spectrum and intensity of X-ray emission from the quiescent sun at intermediate energies (2-30 keV or 6-0.4Å). When this experiment was proposed (early 1965) there had been no reliable measurements of X-ray flux from the quiescent (non-flaring) sun at energies above 3 keV. However, the few lower energy measurements available seemed to indicate that the solar spectrum hardened and the emitting regions became more localized with increasing photon energy.

Excluding direct flare effects, there is no evidence at visible or radio wavelengths to indicate temperatures higher than 2-3 million °K from the normal corona. Regions which emit the yellow line of Ca XV, or "sporadic coronal condensations", exhibit temperatures in the 4-5 million degree range but are commonly observed only over centers of major flare activity. However, the early work of groups at NRL, London-Leicester, and GSFC hinted at the possibility that the X-ray spectrum from the quiescent sun might continue to harden at energies beyond those which had been observed. This seemed to indicate either (1), unexpectedly high temperatures in the outer solar atmosphere, or (2), non-thermal X-ray emission; the latter implying continuous production or storage of energetic electrons on the sun. The series of experiments we are reporting were proposed to investigate these two possibilities, and if possible, to distinguish between them.

We chose to perform the experiment with a large-area array of gas-filled proportional counters mounted with their fields of view nearly normal to the axis of a spin-stabilized Aerobee 150 rocket. Proportional counters were selected as the X-ray detectors because of their high sensitivity and good energy resolution in the spectral region of interest and because of prior experience with this type of system in the laboratory. The spin-stabilized technique was chosen over actively pointing the rocket payload because:

1) The roll-modulated signal simplified background subtraction.
2) It permitted a combination of redundancy and high sensitivity because detectors could be mounted to look out both sides of the rocket.

3) It allowed the possibility of observing sources of cosmic X-rays.
4) The attitude control system was simpler and therefore inherently more reliable.
5) It allowed the instrument compartment to be longer and heavier, and so permitted maximum detector area.
6) The cost of the complete vehicle system was significantly reduced.

In the remainder of this report will be found a narrative description of the three flights and a brief presentation of some instrumental innovations. Following that is a discussion of data analysis techniques and a summary of results to date. Finally, recommendations are made based on knowledge gained as a result of this work. The Appendices contain reprints of publications prepared under this contract.

II. THE EXPERIMENTS

The flight program utilized vehicles designated NASA Aerobees 4.168, 4.169, and 4.248 CS. The first flight, 4.168, took place at White Sands Missile Range on 5 April 1967, eleven months after contract initiation. Further details of the timing and performance of the three flights are given in Table 1.

The design philosophy followed in preparation of the payload was dictated by the character of the X-ray spectrum to be observed. The spectrum at the lower energies was known to fall off steeply with increasing energy, and to be highly variable in intensity. The experimental objective was to extend knowledge of the solar spectrum to higher energies and to provide sufficient overlap at low energies to relate the measurements to earlier work and to contemporary satellite data.

The largest detector area which could be conveniently flown on an Aerobee 150 payload was chosen to achieve maximum sensitivity at high energies. The large proportional counters were filled to the highest gas pressure consistent with satisfactory performance in order to maximize response to the higher energy

Table 1

Vehicle Performance

| | | | |
|---|---|---|---|
| Aerobee Number | 4.168 CS | 4.169 CS | 4.248 CS |
| Date of Launch | 5 Apr. 1967 | 19 Feb. 1968 | 16 Oct. 1968 |
| Time of Launch (UT) | 00:14:59.68 | 23:15:00.39 | 23:14:59.99 |
| Siderial Time | $06^h\ 00^m$ | $02^h\ 06^m$ | $17^h\ 52^m$ |
| Peak Alt. (km) | 160.3 | 157.7 | 154.4 |
| Time of Peak (sec.) | T + 216 | T + 211 | T + 210 |
| Despin Mechanism | Gas | Yo-Yo | Gas |
| Time of Despin (sec.) | T + 227 | T + 215 | T + 199 |
| Duration of Despin (sec.) | 21.5 | $< 1$ | 12.5 |
| Pre-despin Roll Rate: | | | |
| Desired ($^o/_s$) | 720 | 720 | 650 |
| Actual ($^o/_s$) | 670 | 938 | 807 |
| Post-despin Roll Rate: | | | |
| Desired ($^o/_s$) | 80 | 80 | 117 |
| Actual ($^o/_s$) | 78 | 141 | 97 |
| Half-angle of Precession Cone: | | | |
| Pre-despin (deg.) | 5 | 10 | 4.4 |
| Post-despin (deg.) | 33 | 50 | 42 |

X-rays. The detectors, described in more detail below, were equipped with field-shaping electrodes to permit using maximum window area without degradation of resolution. It was also decided to utilize the relatively new technique of pulse risetime discrimination to enhance detector sensitivity by rejecting detector pulses associated with non X-ray background.

Completely filling one side of an Aerobee compartment with an array of large area detectors did not permit the desired degree of redundancy or allow for small-area detectors that were required to record low-energy photons of high intensity. Therefore, identical doors were made on the opposite side of the rocket compartment and supplementary detection systems, as well as two of the three optical aspect sensors and most of the electronics, were mounted there. Figure 1 shows views of both sides of the payload for each of the three flights.

Accurate determination of the form of a steeply falling spectrum is facilitated by a pulse amplitude analysis system having a resolution somewhat better than the resolution of the basic photon detector. It was necessary to record spectra with a time resolution of the order of five milliseconds as the rocket was spinning at approximately two revolutions per second and a longer accumulation time would have resulted in the detectors' fields of view moving too far during one sampling interval. All of these requirements were met by the primary pulse height analyzer which is described briefly in Section III-D below. The technical characteristics of this analyzer are given in more detail in Appendix A.

The pulse height analyzers for supplementary systems were of the stacked-discriminator type. Each energy channel was monitored by an 8-level scaler, with appropriate prescale factor, and was transmitted on an individual PPM telemetry channel. A computer code has been written to process the digital PPM record and output the data in the form of counts per unit time for each channel. This eliminates the need for laborious hand reduction of these data. There were two stacked discriminator systems on Aerobee 4.168 and one such system on each of 4.169 and 4.248.

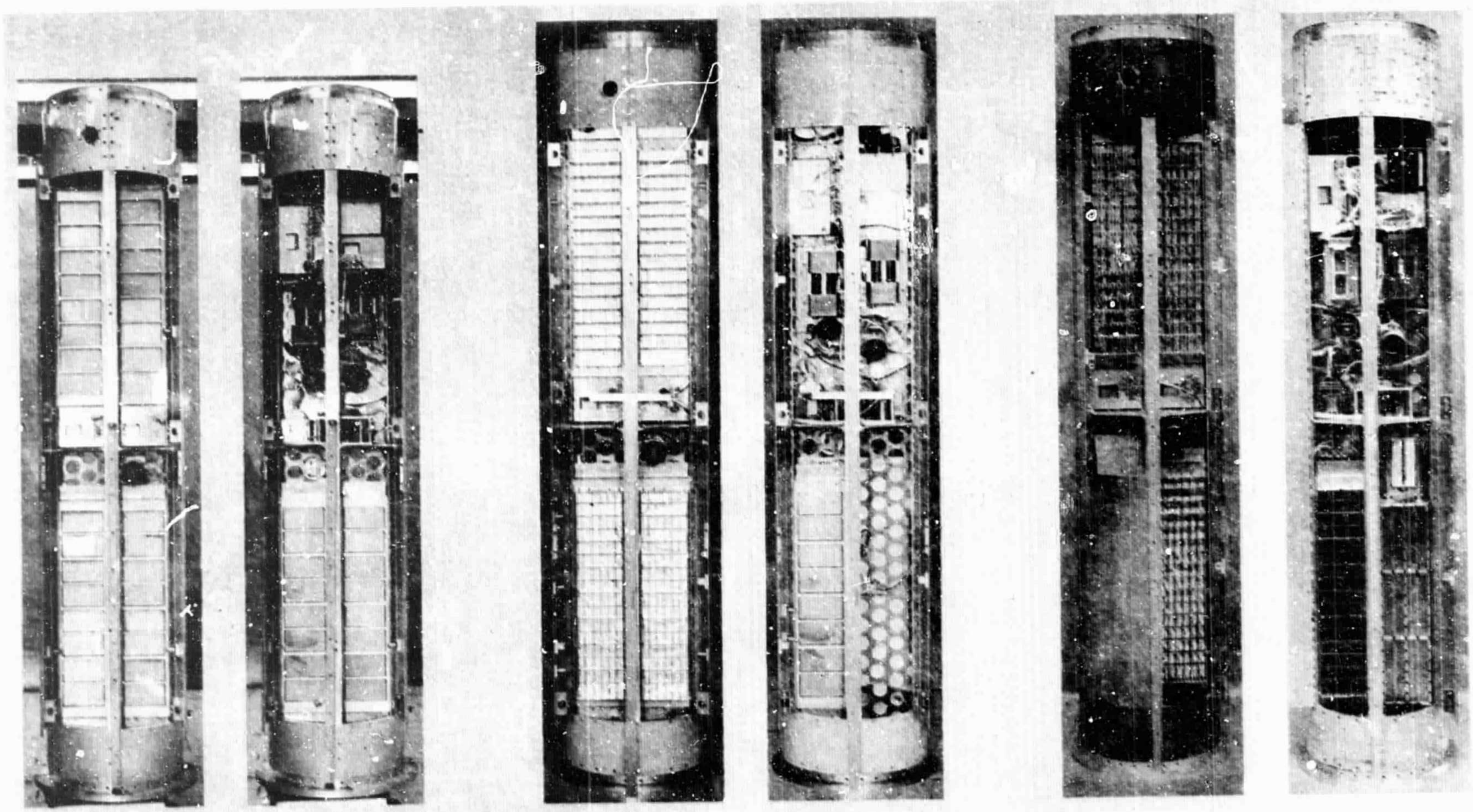

FIG. 1 - Front and back views of the solar X-ray payload as flown on NASA Aerobees 4.168, 4.169 and 4.248 (left to right). A meter stick gives size comparison.

Pulse amplitude information from the low-energy systems was transmitted by a technique wherein individual pulses were stretched in time and telemetered as analog data with the amplitude information preserved. This type of data transmission resulted in appreciable dead time so absolute rate information was derived from logarithmic count rate meters or digital scalers.

In order to obtain X-ray data with the best possible counting statistics, it was necessary to sum the observations over many rolls of the spinning rocket. This required a continuous knowledge of the payload aspect and roll rate which was derived from three solar aspect sensors and two magnetometers. Figure 2 shows the motion of the rocket's roll axis in a zenith and azimuth-angle coordinate system for each of the three flights. Also shown in the figure are the positions of the sun and several other features of interest.

For each flight, the roll axis first precessed on a small cone and then followed a larger cone. This behavior was due to despin of the rocket initiat d near the peak of the trajectory, that was done to aid in reducing the solar data and to cause a more comprehensive scan of the sky.

The instrument calibrations were obtained by monitoring the response of each detection system to X-rays of various energies. These radiations were derived from radioactive sources (principally $Fe^{55}$, $Co^{57}$, and $Cd^{109}$) or fluorescent characteristic X-rays from various elements produced by converting the radiation of a portable X-ray machine. Measurements made with the flight apparatus to determine their dependance on counting rate and photon energy were referenced to equivalent measurements with standard laboratory instruments whenever possible.

Figure 3 gives an example of calibration data taken for the primary system. These particular data are from the pre-flight calibration 248 and were obtained at White Sands Missile Range four days before l . The three peaks are pulse height distributions, (recorded by a laboratory pulse height analyzer) of the response of the entire primary detection system to X-rays of the energies indicated. These data permit direct determination of resolution as a function

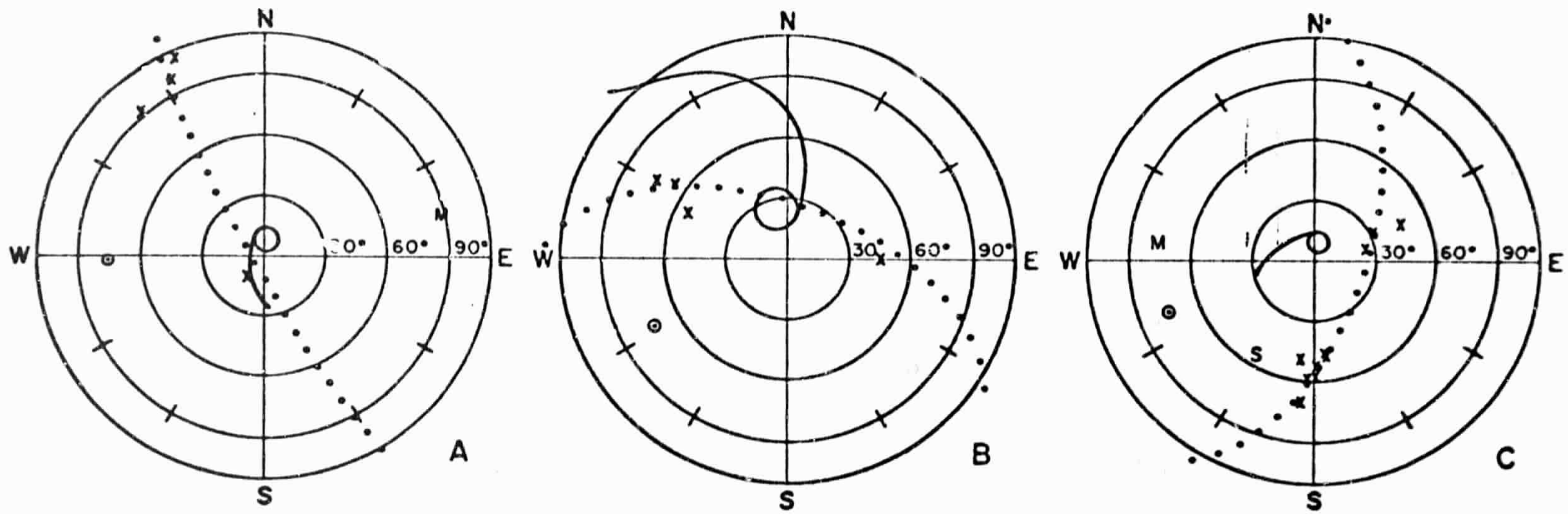


FIG. 2 - Zenith and azimuth angle plots showing the trace of the roll axis throughout the three rocket flights 4.168 (A) 4.169 (B) and 4.248 (C). The position of the sun is indicated by the symbol ⊙, the row of filled circles represent the galactic equator, the position of the radio galaxy M87 is given by the symbol M, the strong X-ray source designated Sco X1 is indicated by S and some other galactic X-ray sources are indicated by X.

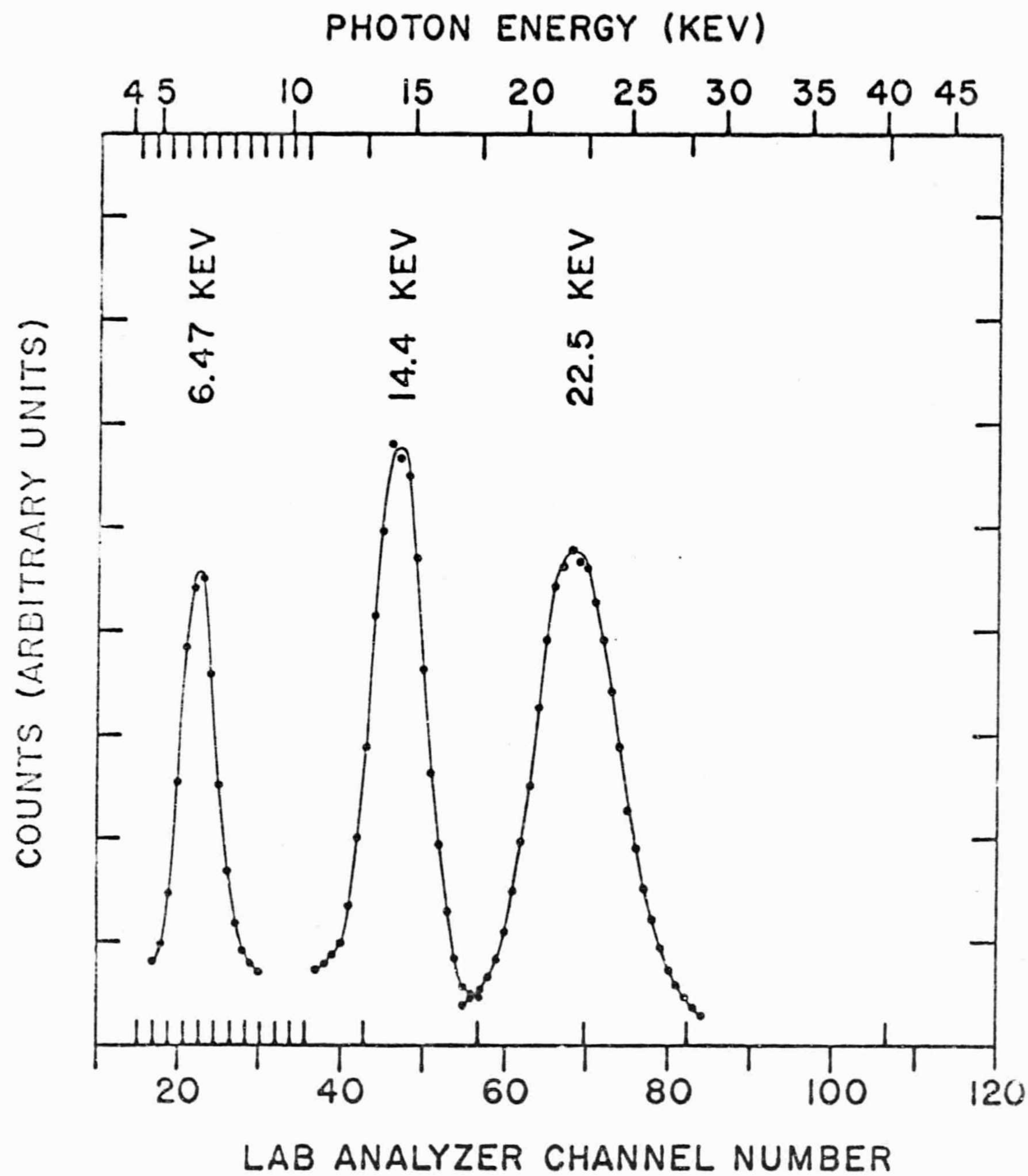


FIG. 3 - Calibration data for the primary X-ray detection system. The pulse height profiles shown were recorded with a laboratory pulse height analyzer when the primary array was irradiated by radioactive sources. Data such as these are used to determine system energy resolution and gain as a function of photon energy. The derived calibration is indicated by the scale at the top of the figure which is given in terms of photon energy and the tick marks top and bottom inside the figure which show the pulse height boundaries of the 16 channels of our primary pulse height analyzer.

of energy as well as system non-linearities with energy. The excellent stability of this system is illustrated by the fact that identical calibration functions could be used for flights 4.169 and 4.248 (which took place eight months apart) with no gain adjustments or other instrumental changes. This implies a system stability of better than two percent.

In-flight calibration was provided by radioactive sources ($Co^{57}$ for 6.47 and 14.4 keV and $Cd^{109}$ for 22.5 keV) mounted on the doors of the compartment. The sources were contained in tungsten cylinders so that the detectors were not illuminated when the doors of the rocket compartment were open. When the doors closed prior to reentry, the sources once again provided calibration information.

Changes made in the payload on each successive flight were based on previous experience and upon the desire to make the most of each flight opportunity. Between flights 4.168 and 4.169 the following changes were made:

1) The five channel stacked-discriminator pulse height analyzer was eliminated in order to make its telemetry channels available for other purposes and because experience with the primary analysis system had demonstrated its reliability in flight.
2) One of the large-area detectors of the supplementary array was eliminated to make space for mounting an optical gating system being tested for use with a source locating collimator to be flown on 4.248. The loss of this counter was no sacrifice as the primary usefulness of this system was at low energies where the flux was high.
3) Collimators ($30^{\circ}$ full width at half maximum) were added to the primary array to decrease the detector solid angleand lower the influence of the signal from diffuse cosmic X-rays. Because this collimation provided more closely defined discrete peaks in the scan direction, a more accurate subtraction of background was permitted.

4) An aluminum filter (0.0048 gm $cm^{-2}$) was added to the primary array to decrease sensitivity of the system to low energy X-rays. The amplifier gain was also decreased to shift the system's lower threshold from 3.75 to 4.25 keV. These changes should have produced a factor of ten decrease in the solar counting rate of this system for a solar X-ray flux equivalent to that experienced during flight of 4.168.
5) Because of difficulties in interpreting data from the primary system under high counting rate conditions the characteristic impedance in the first stage of the double-delay-line clipped linear amplifier was changed. In addition, the logic of the pulse risetime discriminators was altered in order to kill non X-ray pulses in the analyzer, instead of triggering an enable gate for X-ray pulses external to the analyzer. Subsequent results were highly satisfactory.
6) The optical gating system mentioned earlier was installed for test purposes.
7) The cables used to stop the doors when they swung open, and to pull them shut before reentry, were replaced with stronger cables and a better shock absorbing arrangement. (The cables had all broken when the doors opened on 4.168, although no damage resulted since the doors were closed by aerodynamic forces during re-entry.)
8) All TM antennas were moved forward of the severance area so that calibration data could be acquired from all systems during the entire descent of the payload.
9) A telemetry link was installed by NASA to permit closing the payload doors by command from the ground in the event that severance had to occur early due to a low altitude trajectory.

Solar conditions at the time of each flight are summarized in Table 2 and more fully discussed in the section on results. It should be noted that during the second flight (4.169), we observed a solar X-ray enhancement associated with a barely detectable H-$\alpha$ event near the east limb of the sun. This resulted in a peak counting rate 10 times greater than that of 4.168, despite our efforts to reduce the detection sensitivity. Nevertheless, satisfactory data were still obtained from the flight.

Table 2

Solar Conditions

| | | | |
|---|---|---|---|
| Aerobee Number | 4.168 CS[1] | 4.169 CS[2] | 4.248 CS[3] |
| Date of Launch | 5 Apr. 1967 | 19 Feb. 1968 | 16 Oct. 1968 |
| Time at Peak Altitude (UT) | 00:18:30 | 23:18:30 | 23:18:30 |
| 2800 Mc/s Flux (flux units) | 124 | 138 | 137 |
| 8800 " " " " | 294 | 296 | 292 |
| Sunspot Number | 57 | 66 | 89 |
| Daily Avg. 0-8 Å Flux (SOLRAD) | $3x10^{-4}$ | $9x10^{-4}$ | $20x10^{-4}$ |
| Reported Flares during flight | none | none | -F |
| 2-12 Å flux at peak altitude (Explorer 35) (cts/sec.) | - - | 2300 | 1200 |
| Reported radio enhancement | none | none | none |

1) All available satellite and ground data indicate quiet and stable solar conditions.

2) All satellite monitors show declining phase of gradual X-ray enhancement. OSO-4 X-ray telescope shows emission near NE limb (Vaiana, private communication). Examination of H-alpha patrol film shows faint corresponding feature at less than flare brightness.

3) Satellite monitors show sharp burst of X-rays at 2305 UT, lasting only about 5 minutes. Rocket data show X-ray emission varying during flight and locate primary source region near NE limb. H-alpha patrol shows activity in that region but no flare.

A strong upper-atmosphere wind blowing out of the NW caused the initial precession cone of 4.169 to be larger than the cones of the other two vehicles and tilted 25° to the north.

Between flights 4.169 and 4.243 the following changes were made in the payload:

1) The thin-aluminum-window detector was replaced by a new detector system of 25 $cm^2$ area with a thick (1 mm) beryllium window. This was done to more effectively cover the low-energy end of the 2-10-keV range.
2) One of the large-area detectors was removed from the primary array and made into a source-locating detector through the addition of a 7 arc min FWHM collimator.
3) Collimation of the primary array was decreased to 15° FWHM because extra-solar X-ray sources were adjacent to the sun at the October launch time.
4) Aluminum filters over the primary large-area detectors were increased in thickness to 0.014 gm $cm^{-2}$ to further decrease sensitivity to the low energy portion of the spectrum (See Figure 4).
5) Because of variability in solar activity and the possibility of again encountering a high solar X-ray flux, thicker aluminum filters (.0428 and .0063 gm $cm^{-2}$ respectively) were installed over the supplementary large area counter and the new 2-10-keV detector on the day of the flight.
6) Two additional high frequency channels were added to the FM/FM transmitter and an additional commutator was installed to carry data from the source locating detector.
7) Electronics were built to process and store data from the source-locating detector.

In order to avoid a major flare enhancement for the flight of 4.248 real-time communications were maintained up until the moment of launch with an observer visually monitoring the H-$\alpha$ heliograph at Lockheed Solar Observatory and with the USAF Air Weather Service installation at Sunnyvale, California, where real-time data from the Vela satellite net is received and monitored. The extra aluminum filters were installed over the supplementary detection systems as a direct result of the real-time Vela data.

This is an appropriate point to express our appreciation for the splendid cooperation and willing assistance rendered throughout this program by personnel of the GSFC Sounding Rocket Branch, the WSMR launch and recovery crews, and the New Mexico State University Telemetry group.

## III. INSTRUMENTAL INNOVATIONS

In the course of preparing the payloads flown on NASA Aerobees 4.168, 4.169, and 4.248 several new techniques were developed which may be of sufficient general interest to report here.

### A) Payload Compartment

The framework for the compartment is of welded aluminum design with a perforated .250-inch plate, running full length and dividing the compartment along a diameter, providing the basic structural member and a convenient surface for instrument mounting. The screwed-on magnesium skins are entirely removable, providing complete access to the interior of the payload. Each of the four doors is five feet long, hot-rolled to the proper curvature out of .190-inch magnesium, and mounted on standard aircraft-type continuous hinges. The doors which are swung open and held fast by hinge-line springs, were held shut during launch by squib-operated pin pullers and latched shut for re-entry by standard Schlage door latches. This compartment successfully withstood the standard Aerobee bending moment test (maximum deflection was 0.25 inch with a 3000 ft. lb. torque) and is still serviceable after three flights with parachute recovery.

### B) Large Area Proportional Counters

In order to minimize detector weight and permit high temperature bake-out our initial plan was to fabricate the counter bodies entirely from beryllium using aluminum braze techniques. The windows were to be chemically milled and be an integral part of the counter body. Initial efforts with small units were very encouraging but warpage of the pieces during brazing prevented successful fabrication of full-sized units. Electron beam welding was attempted with some success but excessive fabrication cost plus difficulty in obtaining vacuum tight joints caused this effort to be abandoned.

The bodies for flight counters were finally fabricated by dip-brazing components machined from standard rectangular aluminum extrusion. After thorough cleaning and etching, the beryllium windows and high voltage feed-throughs were installed with epoxy resin. Attachments for mounting and end caps were welded to the counter bodies. Figure 3 of Appendix A shows both an assembled counter and component parts of an unassembled unit.

Despite the large cross-sectional area of these counters it was possible to extend the window to within 22mm of the end of the counter without significant loss of gain or resolution by the use of field shaping electrodes. These electrodes, an integral part of the high voltage feed-through, may be seen in Figure 3 of Appendix A.

Overnight vacuum bakeout at 65°C was found to be necessary and sufficient to prepare these counters for filling. They were filled to a pressure of 107 cm Hg (27°C) with commercial P-10 counter gas (.9 Argon + .1 $CH_4$). These counters have shown no significant degradation after 24 months of shelf-life and three flights. Figure 5 shows the calculated photon detection efficiency as a function of energy for these counters and their filters, as they were used on Aerobees 4.168, 4.169 and 4.248.

C) Pulse Risetime Discriminators

The risetimes of pulses produced in a proportional counter are characteristically shorter for X-rays than for non X-ray background radiation. Pulse risetime discriminators (PRD) which used this effect to reduce non X-ray background in the primary detection system were flown on each of the three rockets described in this report. The basic logic involved in the PRD consists of three stages.

1) A delay line differentiation stage which produces a pulse that passes through zero when the detector pulse reaches its peak amplitude.

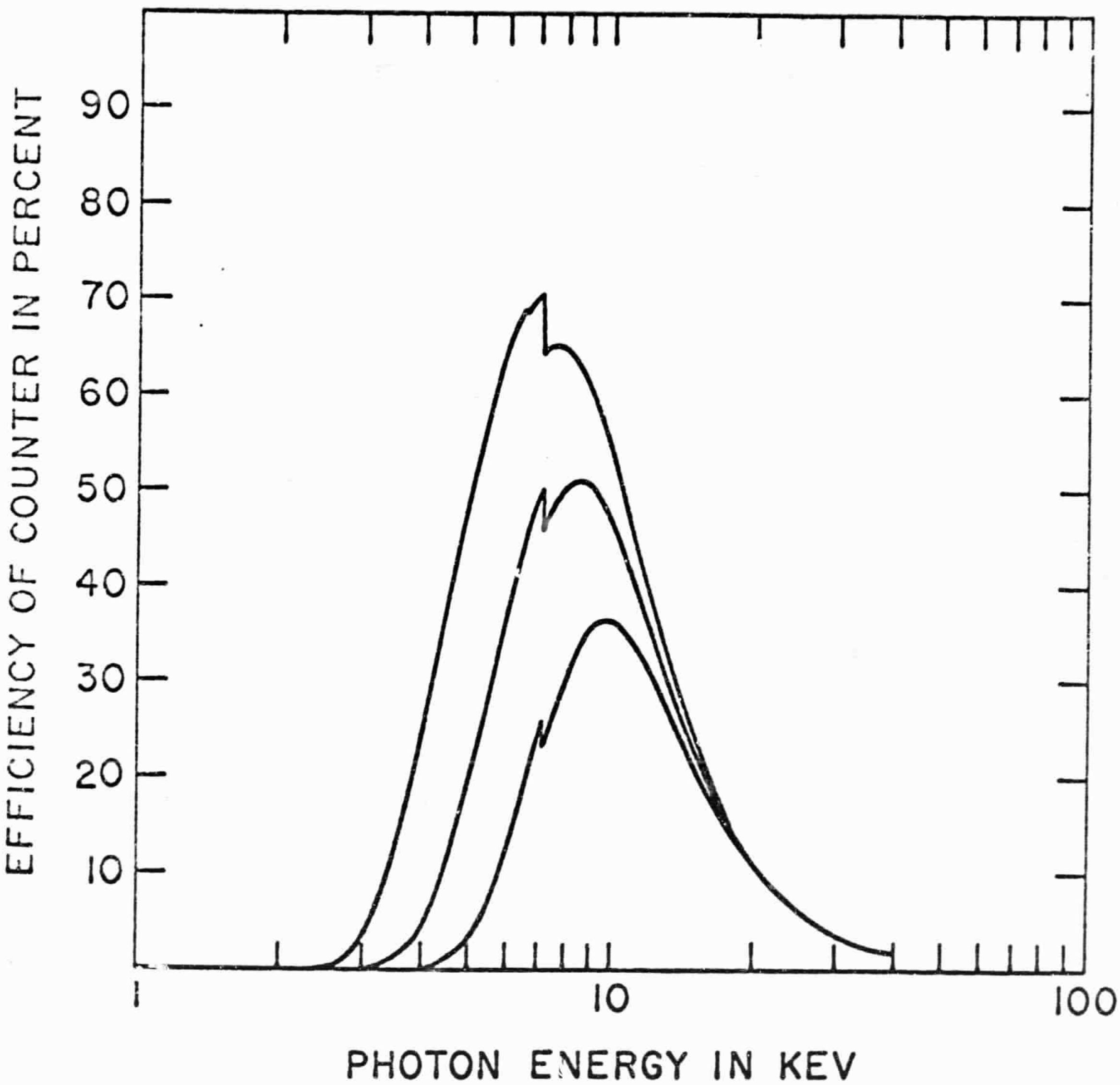


FIG. 5 - Photon detection efficiencies of the proportional counters in the primary array. Upper, central and lower curves refer to flights 4.168, 4.169 and 4.248 respectively. The absorption edge at 7 keV is caused by iron impurity in the window and filter materials.

2) A stage which successively amplifies and diode clips the differentiated pulse. A total amplification of a factor of several hundred is used to produce a nearly rectangular pulse of constant amplitude whose width is equal to the time required for the input pulse from the detector to reach its peak.
3) A stage in which the rectangular pulse goes directly to one half of a coincidence circuit and is also applied to the other half after being passed through a delay line. The length of the delay is adjusted to be slightly longer than the time required for an X-ray pulse to reach peak amplitude. If the time duration of the rectangular pulse exceeds the length of the delay, a coincidence will result, indicating a non X-ray event.

Since the delay line used in the dec 'on making stage is a passive element, the PRD has the advantage of stability at high counting rates. As mentioned earlier the PRD logic was changed between 4.168 and 4.169. This was accomplished by changing from an anti-coincidence circuit in the decision making stage (4.168) to a coincidence circuit (4.169 and 4.248) as described above.

Figure 6a shows the spectrum of room background in one of the large area counters and the reduction obtained with the PRD. The integrated background was reduced 80% by the PRD. A similar reduction was experienced during the flights although no data were obtained on the spectrum of the rejected pulses.

Because of wall and end effects in the proportional counter, X-rays interacting throughout the counter volume produce pulses of varying risetimes. Optimum rejection of background events means that some of the X-ray pulses with long risetimes will also be lost. The fraction of X-ray pulses rejected by the PRD as a function of energy for the flights of 4.169 and 4.248 is shown in 6b. An increase in rejection with energy is expected since more energetic X-rays have slightly longer risetimes. This effect is due to the range of photoelectrons produced by higher energy X-rays becoming comparable to the counter dimensions.

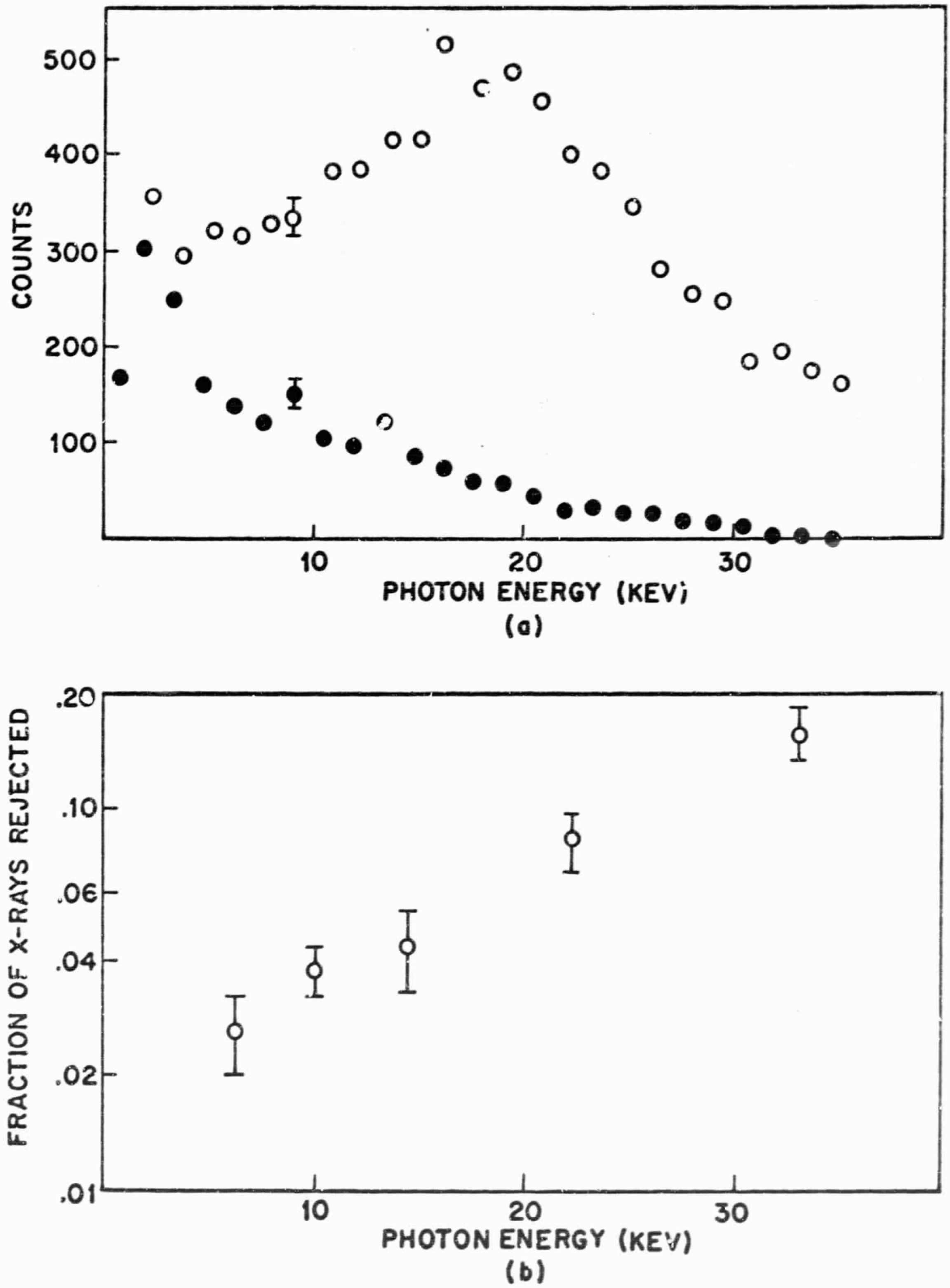


FIG. 6 - Characteristics of the pulse risetime discriminator. In 6a the spectrum of room background radiation is shown both with (open circles) and without (closed circles) the P.R.D. in operation. Fig. 6b shows rejection of X-rays by the P.R.D. as a function of energy as it operated on the flights of 4.169 and 4.248.

D) Primary Pulse Height Analyzer

The pulse height analyzer of the primary system was tailored to the high photon detection sensitivity and inherent energy resolution of the large-area proportional counters.

The unit has 16 differential energy channels whose width increases at higher energy so that a statistically significant number of counts may be acquired from X-ray emitting objects whose spectra fall steeply in intensity with increasing photon energy. The analyzer operates on an analog-to-digital basis with a 3.3 MHz converter clock. The basic accumulation time is 4.75 milliseconds with the 16 channel memory fully buffered for serial readout into telemetry. The digital data wavetrain directly modulated its own FM transmitter at a 20 kilo-bit per second rate. The signal was recorded on the ground either in an "FM record" or "pre-detection" mode in order to preserve the zero reference of the "Non Return to Zero" wavetrain.

IV. EXPERIMENTAL RESULTS

The three rocket flights under this program have produced a large amount of data. The full exploitation of these observations is not yet complete. In the following sections data reduction methods and results of analysis on X-rays from the sun, the Crab Nebula, and the diffuse cosmic X-ray background will be discussed.

A) Data Reduction and Analysis

The following steps were required to reduce the raw telemetered data to X-ray photon flux as a function of photon energy.

1) Aspect Solution: In order to properly sum the counts from a given direction over many rolls of the spinning rocket it was necessary to determine the orientation and angular rates of the vehicle as a function of time for each flight. Figure 2 was prepared from the results of these analyses. A rigid-body approximation proved to be sufficiently accurate to describe the vehicle motion.

2) Preparation of Digital Data: Counting rate information from each detection system has been converted to digital form with timing information preserved. The data from the primary system was received in digitized form and needed only to be converted from telemetry tapes to computer compatible tapes. Digital listings of counts versus time have been prepared.

3) Summation of Data: Versatile computer codes have been prepared which superpose data from many rolls of the rocket while maintaining the proper phase relationships (as determined from the rigid body aspect solution) for the source direction(s) of interest. Figure 7 shows such a superposition of data. For the data from flight 4.169 this program was modified to permit a superposed epoch analysis of the counts from a selected azimuthal interval in order to search for X-ray pulsar emission from the Crab Nebula.

4) Photon Detection Efficiency: Since these observations were integrated over a wide range of aspect angles it was necessary to prepare a code which could compute the photon detection efficiency as a function of photon energy and as a function of aspect angle for an arbitrary proportional counter in the form of a right parallelepiped.

5) Averaging Detection Exposure: It was necessary to compute the appropriately-normalized average product of the photon detection efficiency times the collimator transmission for any source of interest in each set of summed data. This average was computed for 191 energies from 1 to 40 keV.

6) Atmospheric Absorption: In order to utilize some of the high-flux solar data it was necessary to use the atmosphere of the earth as a filter to attenuate the low energy end of the spectrum. Anderson and Francis [J. Atm. Sci., 23, (1966) 110] have made available to us detailed model atmospheres computed for the date, local time and solar activity level of each flight. A code has been written to compute the atmospheric transmission as a function of energy for a given altitude and zenith angle. This code was developed separately and included as a subprogram in the following program.

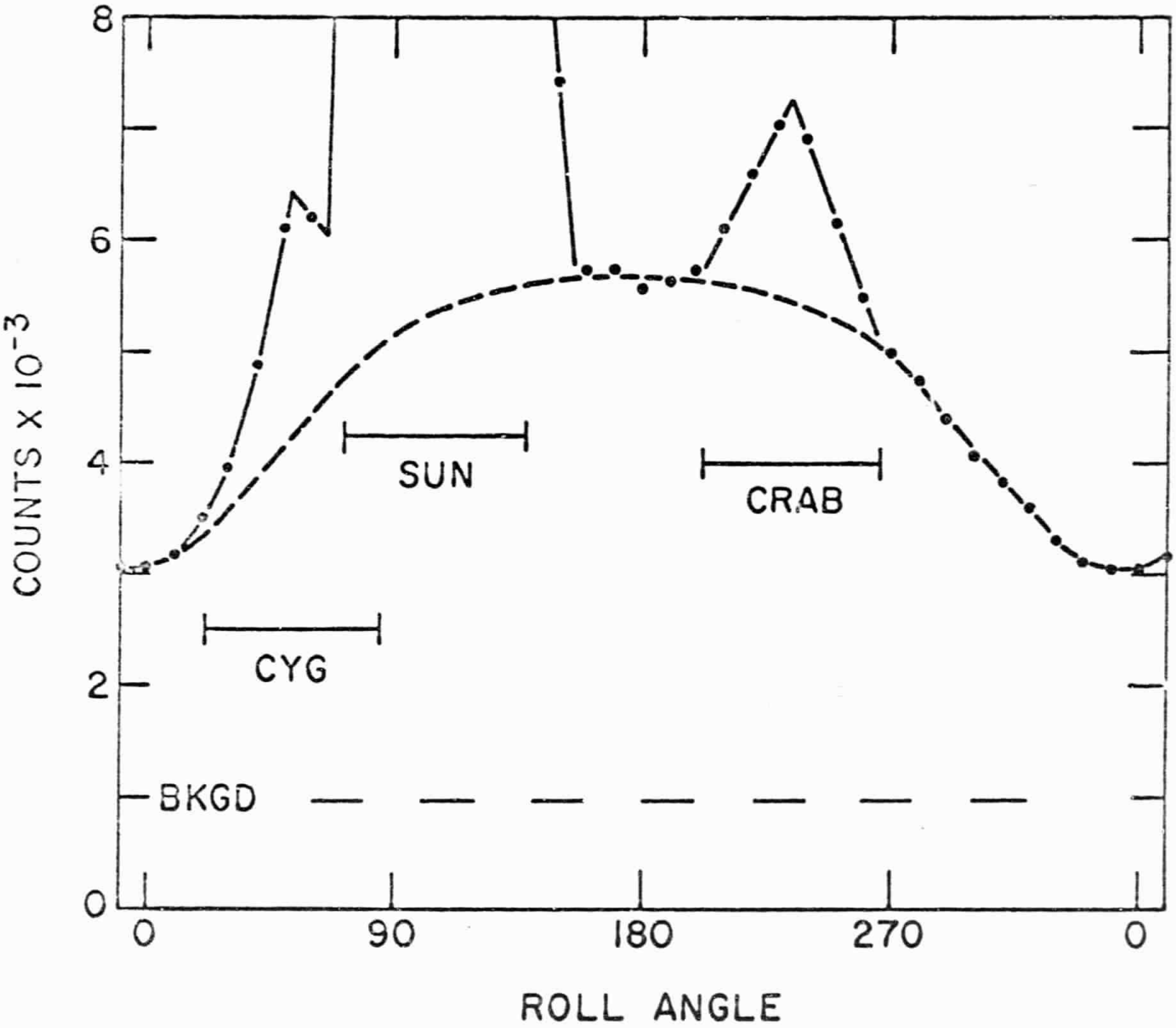


FIG. 7 - An example of data from the primary detection system of Aerobee 4.169 summed over 299 rolls (114.6 seconds) of the rocket before despin. The data points represent counts associated with each $10^{\circ}$ azimuth interval. The horizontal broken line at an ordinate of 950 counts represents non-X-ray counts which were not rejected by the pulse risetime discriminators. This background is about 20% of the total non-X-ray signals recorded by the detectors.

7) X-ray Spectrum Reconstruction: This code computes the predicted number of counts, $N_i$, in each pulse height analyzer channel (photon energy interval) on the basis of the circumstances of the observation, the characteristics and calibration of the detection system, and an assumed incident spectral photon distribution according to the equation

$$N_i = A \times DT \int_0^{\infty} F(E) \times T(E) \times L(E) \times Q(E) \int_{E'_i}^{E'_{i+1}} P(E,E')\, dE'\, dE$$

Where A is the effective detector area, DT is the observing time, F is the assumed photon distribution, T is the transmissivity of the earth's atmosphere, L is the photon loss function of the rise time discriminators (Figure 6b), Q is the averaged detection exposure, and P(E,E') is a Gaussian function representing the energy resolution of the detector or detector array (the width parameter of the Gaussian distribution is determined experimentally, see Figure 3), and gives the contribution at pulse height (energy) E of signals initiated by photons of true energy E'. The integration limits $E'_i$ and $E'_{i+1}$ are set by the lower and upper limits of pulse height analyzer channel i and the other integral is taken over all energies contributing to channel i (formally $0-\infty$).

The weighted difference between the observed and predicted counts in each channel is then computed and the assumed photon spectrum F(E) is adjusted by an iterative, differential, least-squares technique to obtain a best fit to the observations. The program also computes Chi-square and the standard error of the fitted functional parameters.

B) Solar Results

A primary experimental objective of this program was to search for evidence of non-thermal emission in the X-ray continuum of the non-flaring sun. If a hardening of the X-ray spectrum was observed which was greater than could be accounted for on the basis of reasonable thermal models, consistent with radio and optical data, then it could be concluded that non-thermal acceleration and/or storage of particles was taking place within solar centers of activity. Table 2 summarizes the state of solar activity at the times of the three flights.

While the physical interpretation of the solar data is not yet complete, it is possible at this time to answer the primary question posed above. In brief, there appears to be nothing in the solar data from any of the three flights which it is necessary to interpret in terms of non-thermal effects. The data to the contrary in the published results of the first flight (Appendix B) appear to be caused by triple pulse-superposition in the amplifier of the primary system.

Figure 8 reproduces X-ray spectral results from the first two flights, which seem to represent the extremes of our data. These data have been corrected for known instrumental effects and are plotted on a semi-log scale in terms of energy flux. On this scale a simple thermal bremsstrahlung spectrum is approximately a straight line. Although the two spectra are grossly different in amplitude and slope they both appear to be adequately represented by exponential distributions, as indicated. We consider the 4.169 results as provisional because atmospherically attenuated data were used and we have not yet adequately verified our atmospheric absorption correction. However, extrapolation of the spectrum shown to lower energies produces agreement with simultaneous OSO-4 measurements by the X-ray spectrometer of University College London [L. Culhane, private communication].

In order to verify that the emission of energetic solar X-rays is confined to localized regions and to identify the major sources of the observed flux a fan-beam collimator was mounted in front of one of the large area counters for the flight of 4.248. X-ray energies were resolved into two intervals, 2-5 keV and 5-30 keV.

As this detector scanned across the sun the resulting azimuthal distribution of counts indicated one intense source of X-ray emission near the east limb and another weaker source which was located near the central meridian.



LOCKHEED PALO ALTO RESEARCH LABORATORY
LOCKHEED MISSILES & SPACE COMPANY
A GROUP DIVISION OF LOCKHEED AIRCRAFT CORPORATION

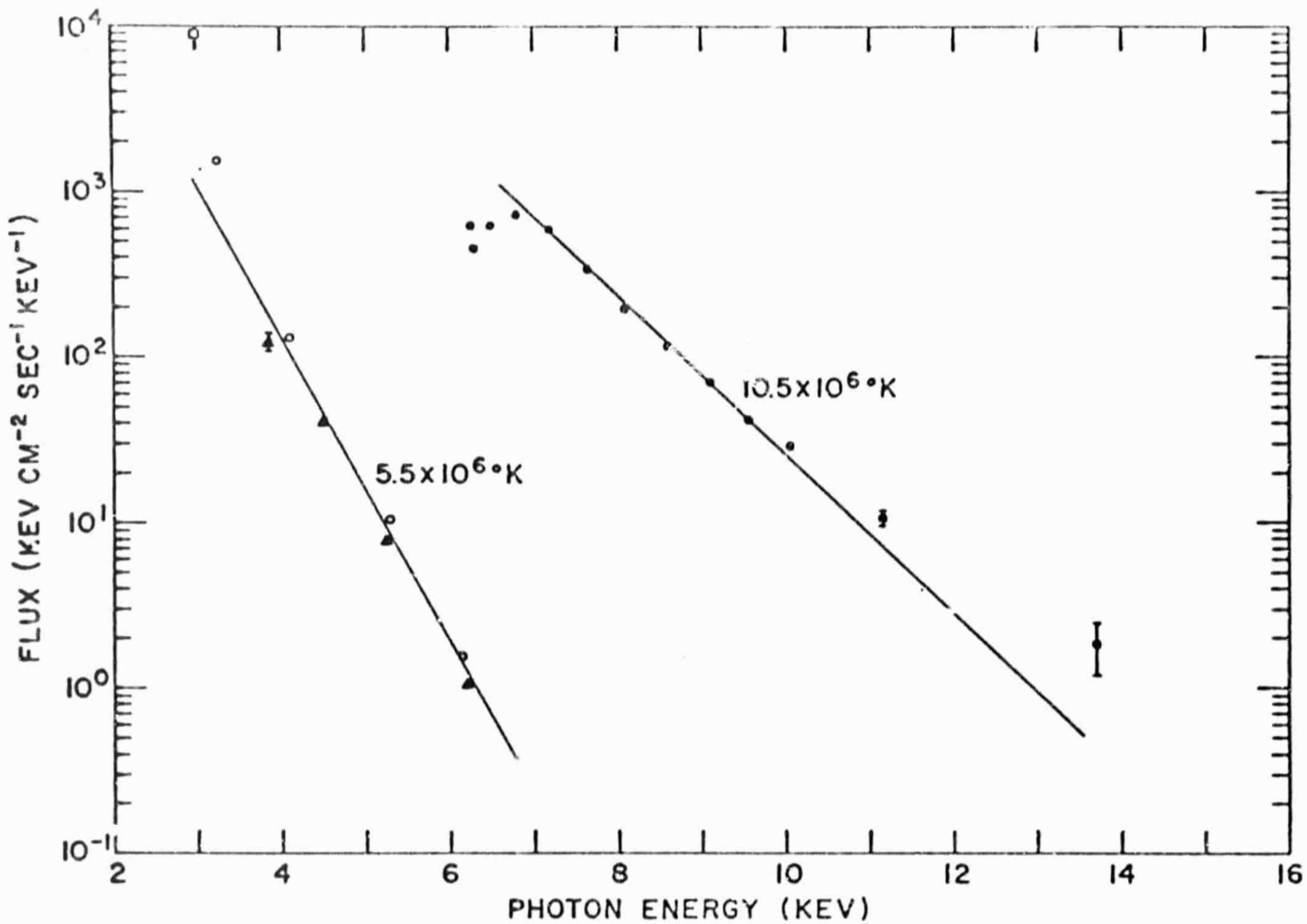


FIG. 8 - Energy spectrum of the solar photons recorded during the flights of Aerobees 4.168 (left) and 4.169 (right) The different symbols represent different detection systems and the statistical counting errors are of the order of the size of the points except where indicated. The electron temperature characterizing the slope of the spectra (on the basis of a thermal bremsstrahlung emission) are given. The 4.169 results are from observations made at a low altitude and atmospheric absorption corrections have been included. In this case the limited number of counts in the lowest energy channels make the data unreliable below 7keV.

The intense source was present in both energy intervals while the weaker source could be resolved from background only in the 2-5 keV channel. The source on the E limb was responsible for more than 90% of the observed solar X-ray emission and can be associated with an active region at N17, E85 which exhibited H$\alpha$ brightening of importance -N at the time the X-ray data were being acquired. For the most intense source the 7 arc-min FWHM collimation places an upper limit of 1-2 arc-min on its angular extent along the scan direction. There are two possible candidates for the less intense source region which are indistinguishable with the available data.

C) The Crab Nebula

During the flight of 4.169 observations of the Crab Nebula were obtained with our primary system. Figure 9 summarizes currently published Crab data; it is evident that our observations are consistent with those of other workers. Subtraction of the large diffuse cosmic X-ray background was the major source of experimental uncertainty in our observations. Figure 7 illustrates the relative amplitudes of the various sources of counts.

Beginning in March 1969 a concerted effort was made to detect a pulsar component to the Crab x-radiation using a superposed-epoch analysis. Calculations indicate that the pulsations should be detectable in our data at about the $3\sigma$ level if 8% of the Crab emission is in the two pulsations per period reported by other workers. So far we have been unsuccessful in our search, but it is premature at this point to use this failure as the basis for concluding that the X-ray pulsar was weaker at the epoch of the flight of 4.169.

D) Diffuse Cosmic X-Rays

The large solid angle and effective area of our primary system, combined with a relatively low non x-ray background and good energy resolution, make it an especially effective instrument for observing the diffuse component of cosmic X-rays. Figure 10 compares our data from 4.169 for a portion of the celestial sphere:

| | |
|---|---|
| Right Ascension | $1^h$ to $4^h$ |
| Declination | $+20^\circ$ to $-70^\circ$ |

with other published measurements of diffuse cosmic X-rays.

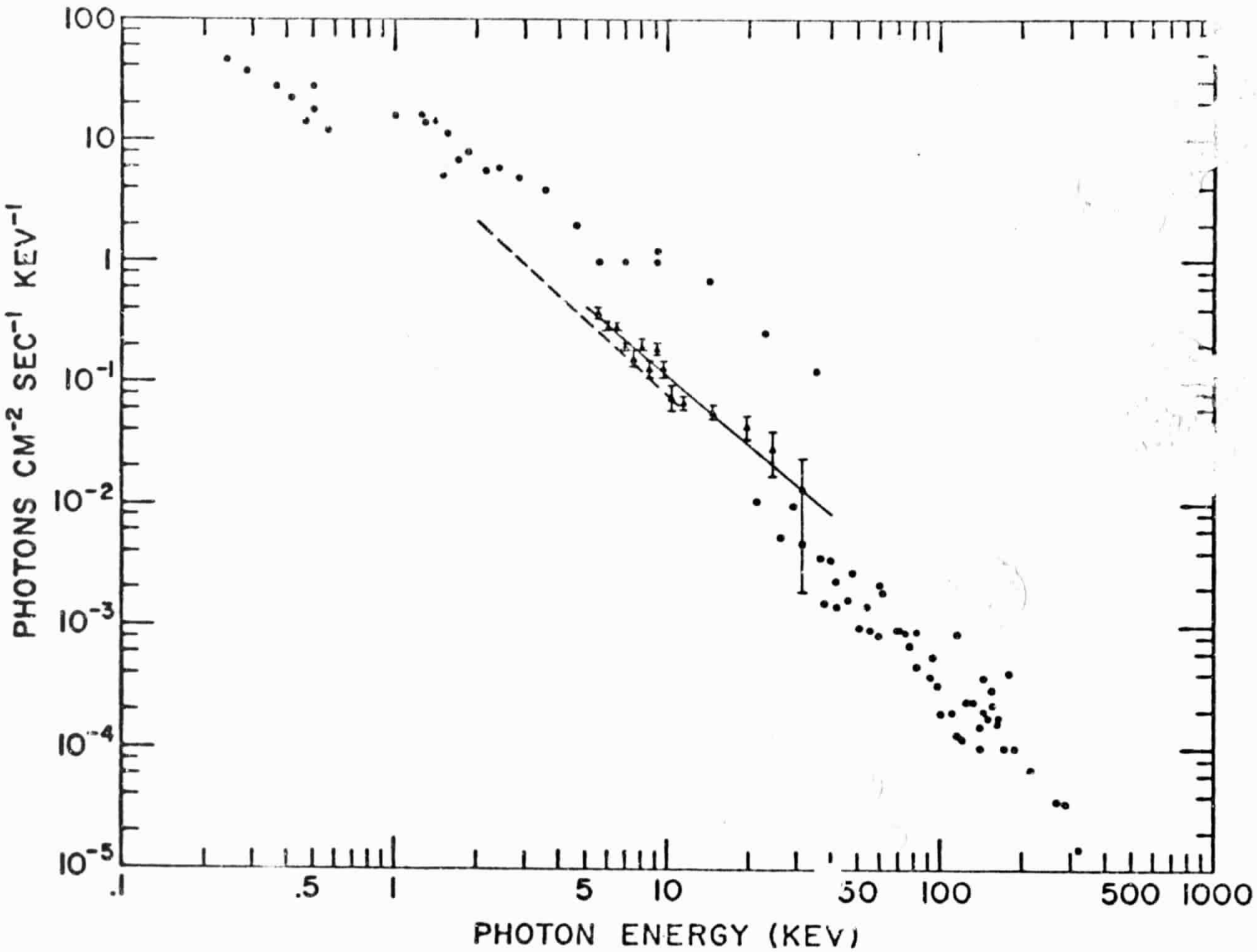


FIG. 9 - X-ray photon spectrum of the Crab nebula. The data from this work are indicated by triangular symbols and the solid line is the best fit power law spectrum of the form.

$$N(E) = 9\,E^{-1.9} \text{ photons cm}^{-2} \text{ sec}^{-1} \text{ keV}^{-1}.$$

Possible systematic errors and errors in background subtraction lead to an estimated uncertainty of ± 0.2 in the spectral index. The plotted error bars are ± one standard deviation and represent purely statistical uncertainties in the source and background data. The filled circles and broken line represent published data of other workers.

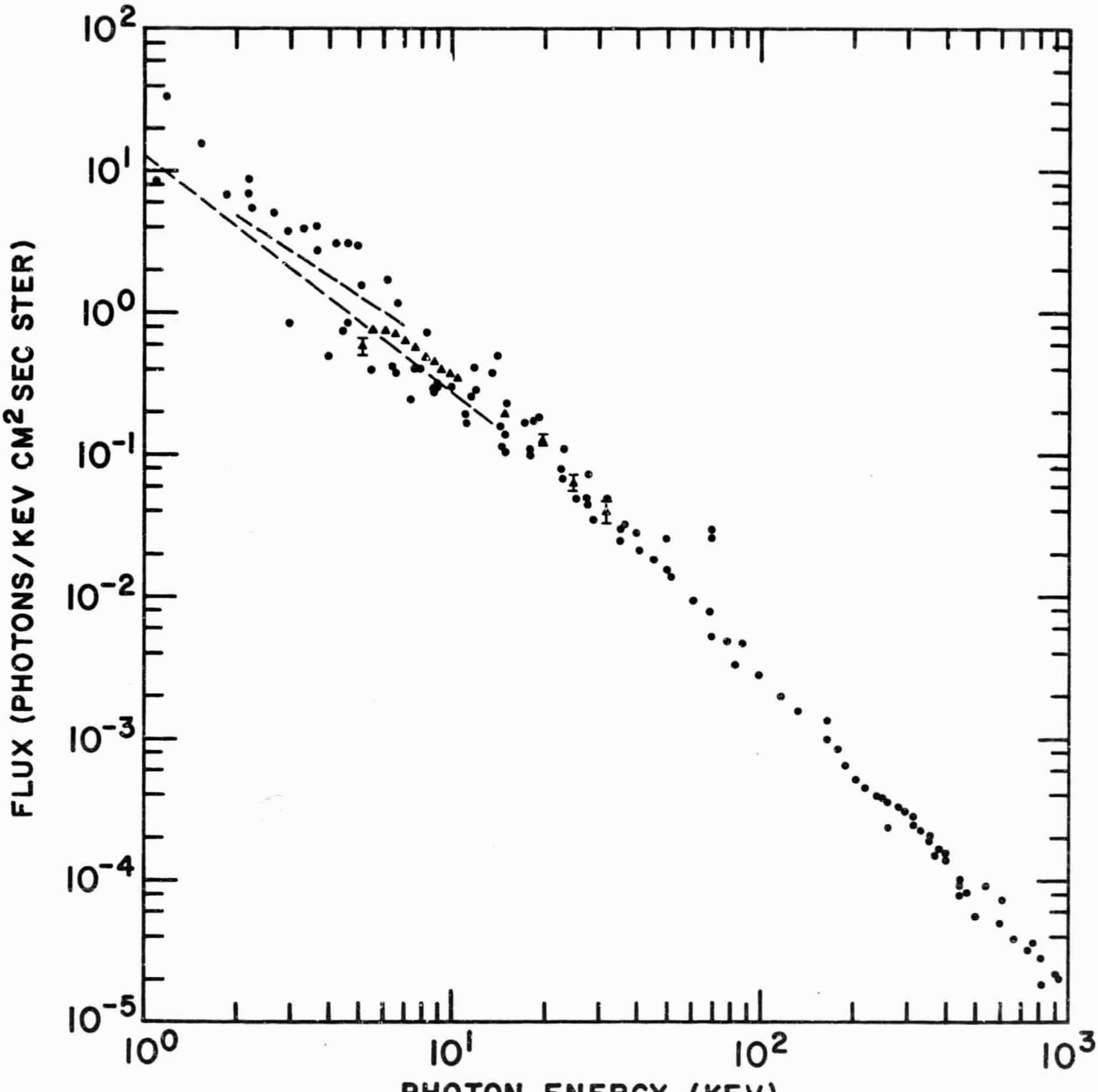


FIG. 10 - X-ray photon sp ctrum of the diffuse cosmic emission. The data from this work are indica ed by triangular symbols. Statistical counting errors are smaller tha the plotted points or are shown. The filled circles and broken lines ar published results of other workers. The sharp turnover of our data at low energies is probably a systematic error related to correction for detector efficiency. The best fit power law spectrum to these data is

$$N(E) = 11\ E^{-1.5} \text{ photons cm}^{-2} \text{ sec}^{-1} \text{ keV}^{-1} \text{ sterad}$$

and does not reflect the break in spectral slope in the 15-20 keV region.

Our raw data have been corrected for non x-ray background (obtained both from earthward-looking detection periods after despin and from data taken between closure of the doors and reentry of the payload) and for a partial transparency of our collimator material at the higher energies. As can be seen from the figure the statistical uncertainties are small.

E) Additional Solar and Extra-Solar Data

This report merely touches upon those aspects of data interpretation farthest along, and in the case of the sun, those which bear most strongly upon meeting the primary objective of this work relative to searching for non-thermal emission from the quiescent sun. We have other data from independent systems which serve to supplement and also to enhance the reliability of these observations. We also have data on other celestial x-ray sources, as has been mentioned in our periodic progress reports. After all of the data (like those presented in Figures 8, 9, and 10) have been further evaluated, we intend to submit the final results and conclusions for formal publication.

## V. CONCLUSIONS AND RECOMMENDATIONS

A) Conclusions

The x-ray emission of the quiescent sun above about 4 keV can be fitted by an exponential function which approximates a thermal bremsstrahlung distribution. The derived temperatures are in general higher than would be inferred from optical or radio data, but beyond this, there is as yet no compelling evidence in these x-ray data for non-thermal effects.

Our x-ray data on the Crab Nebula in the 5-30 keV interval is consistent with that of other workers. An unsuccessful search has been made for a pulsed x-ray component.

The diffuse cosmic x-ray data seem to be well represented by a power law spectrum of the form

$$N(E) = k\,E^{-a} \text{ photons cm}^{-2}\text{ sec}^{-1}\text{ sterad}^{-1}$$

with the spectral index, a, changing from 1.5 to 2.2 within the 15-20 keV energy interval.

B) Recommendations

Further study of the energetic X-ray continuum of solar activity regions is worthwhile. However, to achieve maximum usefulness, future instruments must have collimation to limit the field of view to no more than a few minutes of arc. Because of the extreme variability at these energies, the instrumentation must combine large dynamic range with high sensitivity and good energy resolution. Finally, satellite instrumentation is required in order to adequately study the time variability of the emission. This is necessary information if the growth and decay of active regions is to be understood.

VI. ACKNOWLEDGEMENTS

Many groups and individuals have cooperated in the scientific endeavors of this program. Real-time support at launch and post-flight solar information have been given by the ESSA Space Disturbance Forecast Center, Boulder; Solar Forecast Center, Ent AFB; Sacramento Peak Observatory; High Altitude Observatory; and Lockheed Solar Observatory. Los Alamos Scientific Laboratory has provided X-ray data from the Vela satellites and aided in setting up the real-time X-ray data link through the USAF Air Weather Service Group at Sunnyvale, California, for support of the launch of Aerobee 4.248. The State University of Iowa has provided data from Explorers 33 and 35; OSO-3 data has been supplied by the University of Michigan and the University of California, San Diego.

The American Science and Engineering Company has greatly benefited this program by placing their OSO-4 X-ray heliograph in the operating mode most advantageous to the interpretation of the rocket data and by promptly supplying us with their unpublished observational material for the times of our flights. University College London has provided unpublished X-ray spectrometer measurements from their OSO-4 instrument for the time of the 4.169 flight.

The project scientist has enjoyed a visiting appointment at the Institute for Astronomy, University of Hawaii, during the final period of this contract. His work there was supported by NASA grant NGR 12-001-011.

# A UNIQUE ROCKET-BORNE DATA HANDLING SYSTEM FOR SOLAR X-RAY STUDIES

R. D. Reed, J. C. Bakke, J. B. Reagan and L. W. Acton

Lockheed Palo Alto Research Laboratory
Lockheed Missiles & Space Company
Palo Alto, California

## Summary

A high-speed, high-resolution spectrometer system has been designed for the detection and analysis of low-energy x-rays from a spinning rocket. The system enjoyed a highly successful flight in the spring of 1967 and another flight is currently scheduled for the fall of 1967.

The system was comprised of four large-area beryllium-window proportional counters, an analog pulse-height-to-time converter, a digital data assembler and a complete PCM multiplexer.

The system was capable of analyzing x-ray events at average input rates in excess of 50,000 events per second. The pulse-height-to-time converter, in conjunction with a portion of the digital data assembler, formed a 64-channel pulse-height analyzer and provided an energy resolution of 0.5 keV per channel over the 3-30 keV energy range of the detectors.

The data assembler, using a non-linear, lump digital decoding technique, compiled and stored a complete spectrum on board the rocket. Channel address accumulators were completely buffered so that while one spectrum was being time multiplexed to telemetry, another was being accumulated. This technique gives rise to very short dead-time periods and enabled the detector and pulse-height converter to operate in random-access fashion at high input rates.

The PCM multiplexer portion of the system time multiplexed all of the spectral information, along with absolute rate data, and applicable timing and I.D. information into a serial Non-Return-to-Zero-Level (NRZL) formatted binary output with sufficient drive to directly modulate an FM transmitter. The multiplexer operated from a single, stable 20 kHz oscillator. The timing was such that a complete spectrum, along with rate and timing data, was transmitted each 4.75 milliseconds. A complete frame of 20 spectra, rate and timing signals and all necessary I.D.'s were sent every 0.1 second.

An economical demultiplexer was designed and built for the processing of pre-flight calibration data and for field checkout. This unit accepted the serial wavetrain from the flight instrument and completely demultiplexed it so that the data could be coupled to a standard laboratory pulse-height analyzer for storage, visual display and complete print-out capability. The demultiplexer processed all of the data in a completely digital fashion from the same 20 kHz clock that was in the flight package, so that no D-A and A-D conversion errors were introduced by the demultiplexer or laboratory PHA.

## Introduction

In an effort to gain data that would lead to a better understanding of the physical nature of active regions of the sun, a rocket-borne instrument package was designed and built at the Lockheed Palo Alto Research Laboratory to study the x-ray emissions from these regions in their quiescent state. The experiment was accomplished by launching the instrument package on a spin-stabilized Aerobee rocket from White Sands Missile Range, New Mexico, at 0015 UT on 5 April 1967. The experimental objective of this flight was the measurement of solar x-ray emissions in the 1-30 keV region.

The primary spectrometer of this package, which made spectral measurements of x-rays in the 3-30 keV region, will be described in this paper. The spectrometer consisted of four large-area gas proportional counters whose outputs were parallel coupled to a Pulse-Height Analyzer (PHA) and a Digital Data Assembler and Multiplexer (DDA&M). The PHA and DDA&M were designed as an integral part of the instrument in an effort to realize the full capability of the radiation detectors while maintaining compatibility with the rocket telemetry system. The overall block diagram of the spectrometer is shown in Figure 1.

## Detectors

The radiation detectors used were four large-area gas-filled proportional counters. Each of the four counters had eight windows of approximately 71 $cm^2$ area for a total effective collecting aperture of nearly 0.23 $m^2$ for the entire spectrometer. The windows were of beryllium with a thickness of 0.076 cm and the counters were filled with a mixture of 90% argon - 10% methane to a pressure of 1.4 atmospheres. The computed photon detection efficiency of these counters is shown in Figure 2.

Each counter was equipped with field shaping electrodes so that the gain and resolution were uniform within a few per cent over the entire window area. Figure 3 is a photograph showing the component parts of a counter, including the field shaping electrodes on the HV feed-throughs, as well as one of the assembled counters. The counters were assembled and sealed with epoxy resins and exhibited satisfactory shelf-life and durability.

Each counter was also equipped with its own HV supply, pre-amplifier and a Pulse Risetime Discrimination (PRD) circuit as is depicted in the detector system and PHA block diagram of Figure 4. The PRD circuit differentiated between detector pulses caused by x-rays and those caused by cosmic rays by taking advantage of the fact that in most cases, the cosmic ray produced a more slowly rising pulse[1] This technique proved very effective in reducing the detector background due to cosmic rays.

The output pulses from the four detectors were coupled to the PHA section of the spectrometer via a Double-Delay-Line (DDL) clipped linear amplifier. A linear gate, controlled by the PRD's, followed this amplifier so that only pulses identified as true x-ray signals were delivered to the pulse-height analyzer.

## Pulse-Height Analyzer

The DDL amplifier had a linear bi-polar output signal of approximately two microseconds in total duration. Signal gating of the PHA was accomplished by triggering the threshold and upper level discriminators with the positive portion of the signal from the DDL amplifier prior to pulse-height analyzing the negative portion of the signal. When exceeded, the threshold discriminator triggered a monostable multivibrator which triggered the rate accumulator. This 500 ns wide output was also differentiated and the trailing gate was used as one input to an initiate gate. The initiate gate also had two inhibit inputs, one a "busy" signal controlled by the DDA&M and the other from a monostable multivibrator which was controlled by the upper level discriminator. If the initiate gate were not inhibited, it triggered both a gate-width monostable multivibrator, which opened the signal gate in time to pass the negative portion of the signal from the DDL amplifier, and another monostable multivibrator which signaled the beginning of an analysis to the DDA&M. Those negative signals which passed through the signal gate were amplified and charged a capacitor to a voltage which was linearly proportional to the input-pulse-height. The pulse-height-to-time converter discharged the capacitor in a linear manner while gating on a 3.3 mHz oscillator for the duration of the total discharge time. The gated oscillator output provided the address pulses which were counted in the 64-channel accumulator of the DDA&M.

The total pulse-height analysis time was less than 20 microseconds for the highest level event so the analyzer was capable of analyzing signals at input rates greater than $5 \times 10^4$ counts/sec. At average input rates of $10^6$ counts/sec., the spectrum distortion was less than 10% and was negligible at average rates up to $5 \times 10^4$ counts/sec. The dynamic energy range was set to be approximately 10 for this instrument, although the analyzer was capable of a linear range greater than 30. The basic converter stability was one part in 128 over a temperature range of -40°C to 60°C.

## Digital Data Assembler

The Digital Data Assembler was comprised of an Analysis and Control Logic section, a Spectra Storage section and a Rate Accumulator, while the Multiplexer contained a Bit-Definition Counter, a Word-Definition Counter, a Frame-Division Counter and the Data Merge Control Logic. A block diagram of the Digital Data Assembler and Multiplexer is depicted in Figure 5.

### Analysis and Control

The Analysis and Control Logic (ACL) section of the spectrometer is where most of the dynamic decisions were made which concerned the analysis of the x-ray events. The ACL section utilized three inputs from the PHA section, an analysis start pulse, an analysis envelope pulse and an analysis pulse train. The analysis control logic then furnished the "busy" inhibit signal gate, coupled the analysis pulse train to the 64-channel binary accumulator, provided the decoder strobe pulse which controlled the address decoding process, reset the 64-channel accumulator, and removed the inhibit command from the signal gate when the analysis was complete. The 64-channel binary accumulator, which counted the analysis pulse train, provided an energy resolution of 0.5 keV per channel over the 3-30 keV energy range of the instrument.

### Spectra Storage

When a decoder strobe pulse was received from the analysis control logic, the address decoder presented a single pulse to the input of one of the address storage accumulators. Because of weight, power, volume and cost constraints, only 16 address storage accumulators were used to cover the dynamic energy range of the analyzer. Since maximum resolution was desired in the 3-8.5 keV region, and because flux in the region above 8.5 keV was anticipated to be lower than in the region below 8.5 keV, a non-linear, lumped decoding technique was used. The decoder weighting was such that a one-to-one correspondence existed between the primary analysis channels, 1 through 11, and the address storage locations, 1 through 11. The remaining channels were non-linearly lumped. The channel-to-channel correspondence and equivalent energy levels are shown in Figure 6.

Each of the 16 address storage accumulators was a 5-bit binary counter, and each accumulator was buffered with a 5-bit register. The data in each address accumulator were broadside shifted into the address buffer register upon command from the Data Merge Control (DMC) section of the multiplexer. All accumulators shifted their data into the buffers and were cleared simultaneously.

Each buffer register was then sequentially scanned and a 5-bit word describing the contents of each register was presented to the DMC unit in the multiplexer. While the registers were being scanned and output words were being formed, the address accumulators were able to accept new data and form a new 16-channel spectrum. There was essentially no dead time introduced into the system by the address storage portion of the system since the data shift, which was accomplished broadside, required less than 60 ns and took place only once per transmitted spectrum.

## Rate Accumulator

Also included in the DDA section of the instrument was a 10-bit rate accumulator and scanner. The rate accumulator was a binary counter which accepted pulses from the rate multivibrator in the PHA. The rate accumulator counted every input signal whose amplitude was higher than the lower threshold regardless of the presence of an overload signal or busy inhibit. The rate accumulator was not buffered, but scanned directly so that it was necessary to inhibit the input while the output word was being formed. This amounted to an "off" time of only 10% of the total possible accumulation time, and was completely constant and periodic.

The rate data was used to normalize the spectral data. The instrument was able to completely analyze an average of 50,000 x-ray events per second without appreciable distortion, and had storage capability of over 100,000 events per second.

## Multiplexer

The basic bit rate of the multiplexer was 20 K-bits per second. The system clock was a very stable 20 kHz oscillator which had two isolated outputs. One of the outputs was used only for ground checkout, while the other was fed to the bit-definition counter. The bit-definition counter was a mod-5 counter which, with its decoder, defined 5 discrete periodic bits for use by the DMC and Sync Pattern Generator (SPG).

The first bit was also coupled to the word-definition counter, which was a convertible mod-19/mod-27 counter. In its normal mode, the word-definition counter and its decoder defined 19 discrete word-length pulses for use by the DMC & SPG. In its alternate mode, the word-definition counter defined 27 word pulses.

The first word pulse was coupled to the frame-division-definition counter, which was a mod-20 counter. The mod-20 counter and its decoder defined 20 divisions of each main frame of the multiplexer. Using these 20 time-discrete functions, the mod-20 decoder controlled the operating mode of the convertible mod-19/mod-27 word counter. The complete 5-bit output of the frame-division decoder was also fed to the DMC where it was used as a frame-division I.D. word.

The first frame-division pulse was also used to increment the frame I.D. counter, which was a 10-bit binary unit. The frame I.D. counter was supplied with a scanner which, upon command of the DMC & SPG, furnished 10 bits of incremental frame count to the DMC for formatting.

The DMC, using the various inputs from the bit-definition decoder, the word-definition decoder and the frame-division decoder, formed all of the control signals that were used to sequentially interrogate all of the data scanners. The DMC & SPG also takes all of the data from the various sources and formats them into a single serial Non-Return-to-Zero (NRZ) wavetrain with the necessary I.D.'s and frame synchronization pattern inserted in their proper places in the frame.

## Format

As previously mentioned, the instrument output was a serial, binary-coded NRZ wavetrain with a basic bit rate of 20 K-bits per second. Each frame consisted of 388 five-bit words and required a period of 97.9 milliseconds for presentation. Each complete frame was made up of 20 frame divisions, with the first 19 frame divisions containing 19 words each, while the 20th frame division contained 27 words.

As depicted in Figure 7, the data allocations were as follows: words 1 through 16 of all 20 frame divisions described spectral data, words 17 and 18 were allotted to absolute rate data, while word 19 was the frame division I.D. In addition, frame division 20 contained 8 unique words. Words 20 and 21 of this frame division were the frame I.D., while words 22 through 27 contained the sync pattern.

The general formatting and timing described above shows that a complete 16-channel spectrum from 3-30 keV, along with the absolute rate data and timing identification, was telemetered each 4.75 milliseconds.

The synchronization pattern consisted of the following 30-bit code:

111110101111001100110100000000.

This code was chosen from the work of J. L. Maury, Jr. and F. J. Styles[2] and demonstrates a high degree of reliability for recognition of the true sync pattern while rejecting false patterns.

## Ground Support Equipment

The nature of the data and its formatting makes computer reduction ideal, and the flight data was reduced using a digital demultiplexer and computer as outlined in a previous paper[3]. However, due to the high data rates, checkout and calibration of the instrument at locations which were remote from a computer were impossible without some special equipment. To overcome this problem, a low-cost special demultiplexer was designed and constructed. This demultiplexer, in conjunction with a standard laboratory pulse-height analyzer and a printer, formed all the necessary checkout equipment for the flight instrument. A block diagram of this demultiplexer is shown in Figure 8. The 20 kHz clock signal was derived from the primary bit-rate clock in the flight instrument and was used both for the data shift signal and to increment the bit-rate counter.

The serial NRZ data were continuously entered into a 30-bit serial shift register by the 20 kHz clock signal, while a 30-bit sync comparator continuously scanned the data register for the sync pattern. When a sync recognition was made by the comparator, a reset signal was generated and coupled to the bit-definition counter, the word-definition counter and the frame-division counter, where the respective timing counts were set to bit one, word one and frame division one.

The outputs of the word counter and the frame-division counter formed the required signals to control the lab PHA and also the data conversion system. The lab analyzer which was available for this use had no provision for parallel access to its memory. Therefore, the data from the flight instrument had to be converted to some other form. To overcome this problem, the demultiplexer converted the data, which represented the number of counts stored in a spectral channel, into the prescribed number of serial pulses and entered these into individual address locations in the lab PHA.

The lab PHA was operated in the multiscaler mode, with 17 address channels being used for storage of the spectrometer data. Channels 1 through 16 were used for storage of spectral data, while the rate data was entered into Channel 17. The Conversion and Storage Control (C&SC) section of the demultiplexer furnished the channel advance, channel dwell and reset signals to control the lab PHA.

When a spectral data word was in the proper position in the main 30-bit register, its numerical inverse was parallel shifted into a 5-bit register upon control by the C&SC. A slow oscillator was then gated on and its output coupled to the 5-bit register, which now operated as a straight binary counter. The oscillator output was also fed to the lab PHA, which counted the pulses and stored that count in a single address storage location. As the count in the 5-bit register was incrementally increasing, the register was scanned by a maximum count detector, which shut off the oscillator when the count in the register reached all ones.

As an example, consider that the data word in the main 30-bit register was 01000, with least significant bit to the right. The number 10111 was then shifted into the 5-bit register and exactly 8 clock pulses were required to reach a count of 11111 in the 5-bit register. Since the oscillator was also fed to the lab PHA, 8 pulses would be counted and entered into a memory location there, with that location uniquely corresponding to the transmitted spectral channel.

When the rate words were in the proper position in the main 30-bit register, their numerical inverse was shifted into the pair of 5-bit shift registers. The same procedure as was used for the spectral word followed, except that a fast oscillator was chosen in order to send the correct number of pulses to the PHA in the available length of time. In this mode, the two registers acted as a single 10-bit binary counter.

After accumulating data from the flight instrument for a time that was sufficient to provide good statistics, the demultiplexer operation was inhibited and the spectrum that was stored in the PHA memory was printed out using an auxiliary printer.

## Calibration and Data

The flight instrument was calibrated in the laboratory using standard x-ray source techniques. For in-flight calibration of the instrument, a small $Co^{57}$ source was mounted in front of each of the detectors on the payload chamber doors. The chamber doors were mechanically opened to allow the detectors to view the sun after the first 71 seconds of flight and shut again just prior to re-entry, giving both a pre-data and post-data calibration. The 6.4 keV and 14.4 keV x-ray lines from this source provided an excellent in-flight calibration.

Figure 9 represents the raw data that was stored in 3 channels of the spectrometer during 176 revolutions of the spinning rocket. It should be noted that at the time of the flight, the sun was in the West at a zenith angle of approximately 75°. The width of the solar peak corresponds to the detector field of view in the direction normal to the spin axis of the rocket and the variation of the data in the non-solar regions is caused by other x-ray sources. These data provide more detailed information on the quiescent solar spectrum, in the 3-30 keV region, than was previously available, and a preliminary report of the data and conclusions obtained from this flight is being published elsewhere[4].


## Acknowledgements

The authors wish to acknowledge the valuable assistance received from Dr. R. C. Catura and Messrs. W. G. Soltwedel, J. D. Matthews, H. Uyeda and V. Olivier in the design and fabrication of this instrument.

This instrument was developed with the support of both the National Aeronautics and Space Administration, under Contract NASw-1398, and the Lockheed Independent Research Program. Their support is greatly appreciated.



Fig. 1. X-Ray Spectrometer System Basic Block Diagram

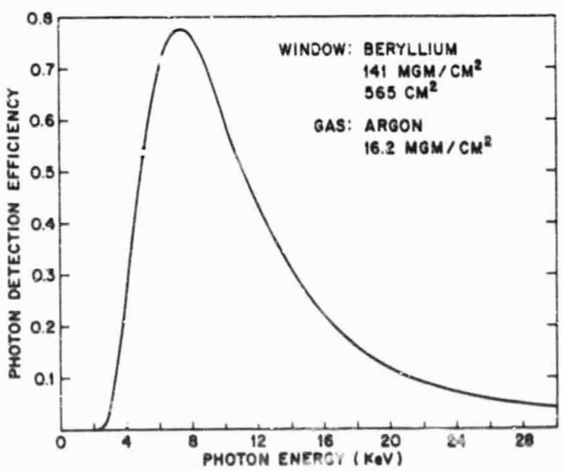


Fig. 2. Computed Photon Detection Efficiency

## References


1. "Pulse Shape Discrimination in Proportional Counters," E. Mathieson and P. W. Sandford, Proceedings, International Symposium on Nuclear Electronics, 65, 1963.

2. "Development of Optimum Frame Synchronization Codes for Goddard Space Flight Center PCM Telemetry Standards," J. L. Maury, Jr. and F. J. Styles, Proceedings of the 1964 National Telemetering Conference, Session II-1, 1964.

3. "A Versatile Satellite Data-Handling System for Space Radiation Measurements," J. B. Reagan, R. D. Reed and J. C. Bakke, IEEE Transactions on Nuclear Science, NS-14, No. 1, 620, 1967.

4. "Observations of X-Rays from Quiescent Solar Active Regions," L. W. Acton and P. C. Fisher, Proceedings of IAU Symposium No. 35, The Structure & Development of Solar Active Regions, Reidel Publ. Co., Holland (to be published, 1968).


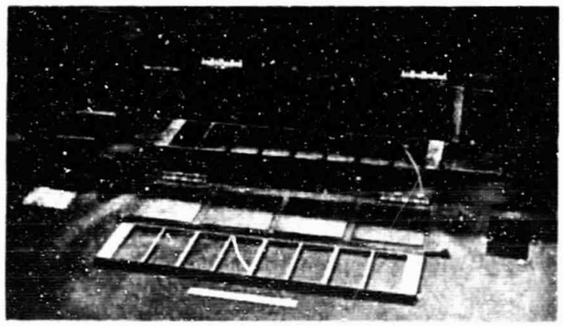

Fig. 3. An Assembled Detector With Associated Component Parts

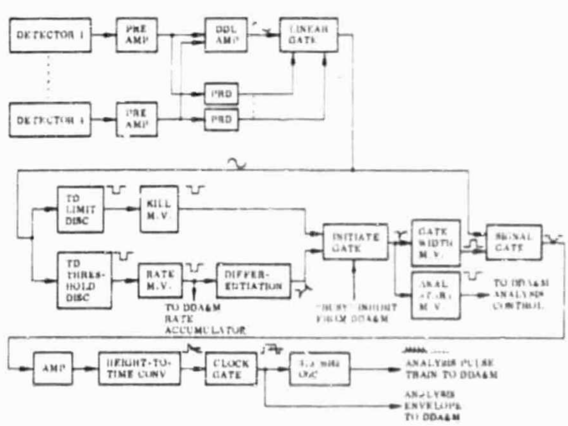


Fig. 4. Detector System & Pha Block Diagram

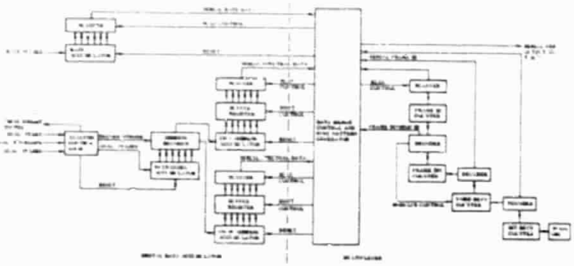

Fig. 5. Digital Data Accumulator & Multiplexer Block Diagram

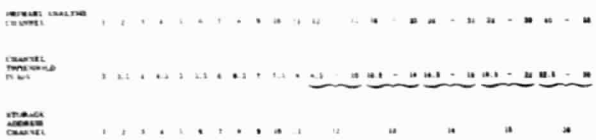

Fig. 6. Address Decoder Weighting

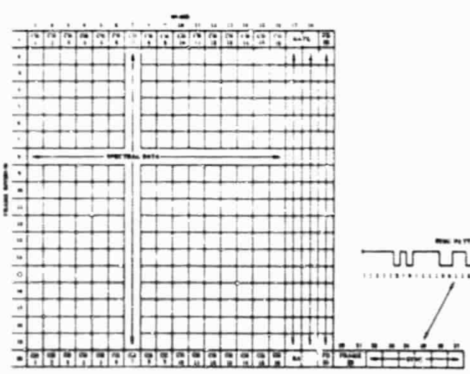

Fig. 7. Data Format

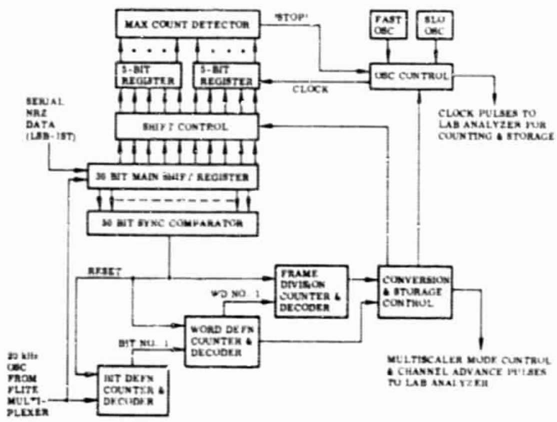


Fig. 8. Demultiplexer Block Diagram

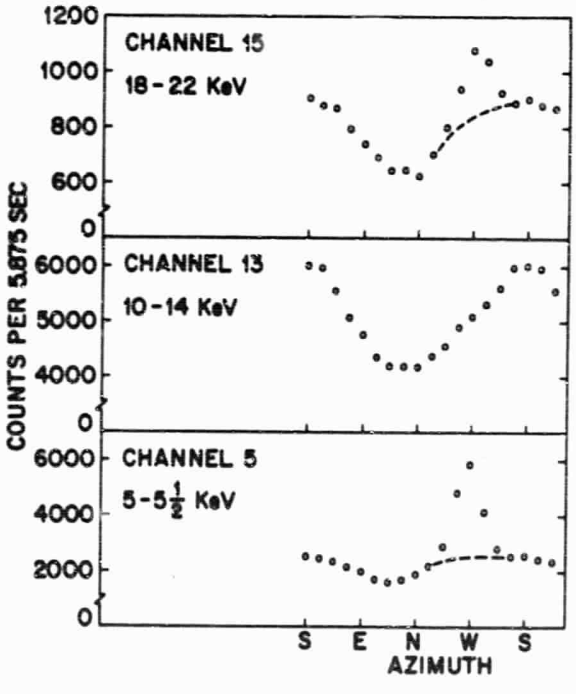


Fig. 9. Typical Flight Data of 3 Channels Showing Azimuthal Distribution

# OBSERVATIONS OF ENERGETIC X-RAYS FROM QUIESCENT SOLAR ACTIVE REGIONS*

LOREN W. ACTON and PHILIP C. FISHER**
*(Lockheed Palo Alto Research Laboratory, Palo Alto, Calif., U.S.A.)*

ABSTRACT

A measurement of the solar X-ray spectrum in the 1–30 KeV interval was made by rocket-borne instruments at 0015 UT on April 5, 1967. These measurements show that the solar X-ray spectrum, which falls off steeply with energy below 4 KeV, becomes less steep above this energy. These data are taken to indicate that energetic, non-thermal, electrons are present or continuously produced in quiescent solar active regions. No optical flare activity was reported for several hours around the time of these observations.

## 1. The Experiment

A solar active region represents a remarkable concentration of energetic phenomena exemplified by the tremendous outpouring of energy associated with solar flares which, although long recognized, still remain to be understood. A study of the quiescent state of active regions can advance our knowledge of the physical nature of such regions and hence the sources of flare energy.

An experiment to investigate the quiescent state of solar active regions was carried out by instruments flown on a spin-stabilized rocket, which was launched from White Sands Missile Range, N.M., at 0015 UT on April 5, 1967. The nose of the spinning rocket was pointed approximately at the zenith with a yaw cone having a half angle of about 5°. X-ray detectors were mounted so as to look out the sides of the rocket. The Sun was located in the West at a zenith angle of approximately 75°. The experiment did not provide any information concerning the positions of the X-ray sources on the Sun. However, recent X-ray photographs of the Sun (Giacconi *et al.*, 1965; Pounds and Russell, 1966; Underwood and Muney, 1967; Zhitnik *et al.*, 1967) seem to establish conclusively that the emission of the harder X-rays is restricted to centres of activity.

The object of the experiment was to measure the solar X-ray emission in the 1 KeV (12 Å) to 30 KeV (0·4 Å) region. The radiation sensors were eight gas-filled proportional counters with a total area of 0·34 $m^2$. The signals from these proportional

* This work has been supported by the National Aeronautics and Space Administration under contract NASw-1398 and by the Lockheed Independent Research Program.
** Presented by L. W. Acton.

counters were processed by five different pulse-amplitude measuring systems which were equipped with a variety of provisions for reducing the deleterious effects of the cosmic-ray environment. The primary instrument, which yielded the most precise measurement of the solar X-ray spectrum, consisted of four proportional counters of total area 0·23 $m^2$. Figure 1 illustrates the computed photon-detection efficiency

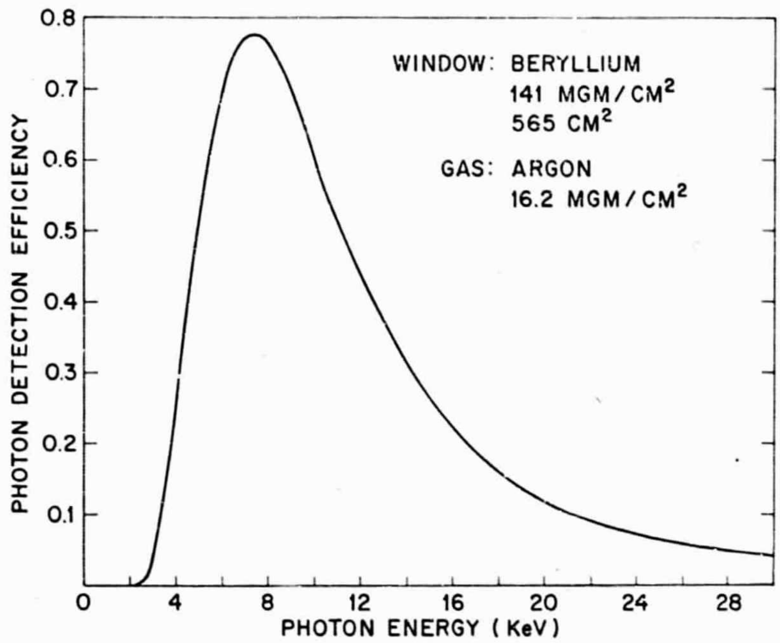


FIG. 1. *Typical photon-detection efficiency of the proportional counters used in the primary system. Four such counters were used to feed the primary pulse-height analyzer. The energy resolution (full width at half maximum) of these counters at 6 KeV was better than 20% over the entire window area.*

of each of the four counters of the primary instrument. These counters were equipped with field-shaping electrodes so that the gain and resolution were uniform to within a few percent over the entire window area. Pulses from these counters were fed into a single analog-to-digital pulse-height analyzer which was developed specifically for this experiment (Reed *et al.*, 1968). The analyzer was designed so that high pulse rates could be handled and a complete 16-channel spectrum was read out every 5 milliseconds, with no dead time introduced by the read-out process. The channels of this analyzer were arranged so that the channel widths in the 3–8·5 KeV interval were approximately 0·5 KeV. The higher energy channels were set wider because of the anticipated lower photon flux at these energies. A very important feature of this X-ray detection system was a pulse rise-time discrimination circuit which rejected a high percentage of the pulses produced in the proportional counters by cosmic rays while accepting the pulses produced by X-rays. This circuit was developed especially for this experiment by Dr. R. C. Catura of this laboratory. The technique was first used by Mathieson and Sanford (1963).

## 2. The Data

It is important to emphasize that the following discussion of the experimental results represents a preliminary analysis of the data from the flight. The possibility exists that systematic errors remain, both in our understanding of the performance of the instruments and in the data-reduction techniques which have been used. However, the internal consistency of the initial reduction of these data is such that preliminary conclusions may be drawn at this time.

Figure 2 presents examples of the azimuthal distribution of detector counts recorded in three different pulse-height intervals, or channels, of the primary instrument. These data were acquired in 94 sec and represent a sum over 176 rolls of the spinning rocket.

Most of the non-solar or 'background' signal is caused by diffuse cosmic X-rays and unresolved cosmic X-ray sources. The sinusoidal variation with azimuth of this signal is introduced by the tilt, toward the North, of the rocket roll axis. Channels 5 and 15 have a distinct maximum in the West, the position of the Sun at the time of the flight. The data in the figure have not been corrected for system dead-time.

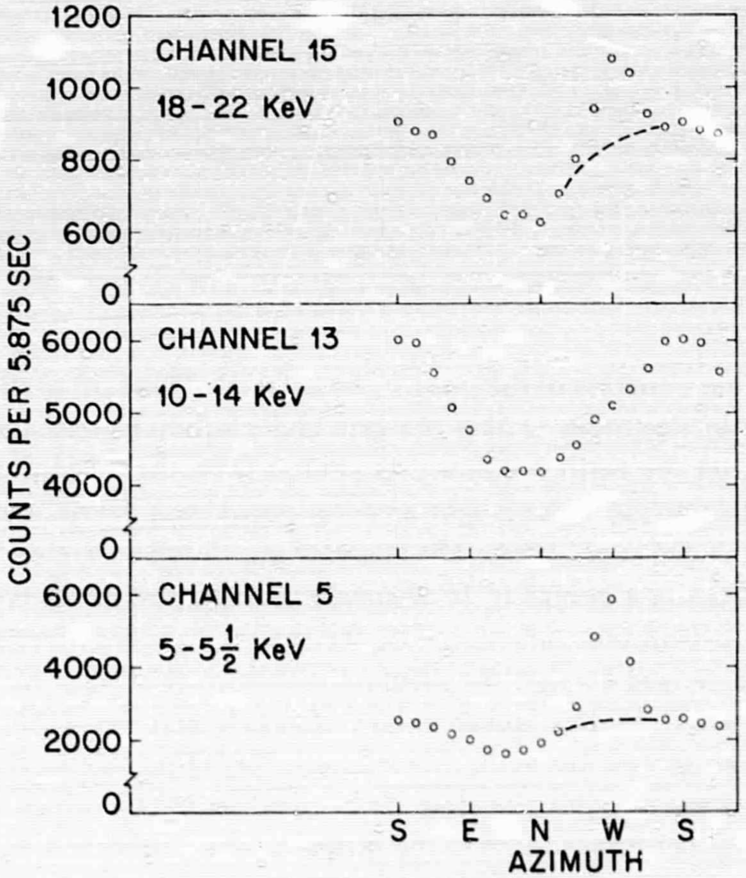


FIG. 2. *Azimuthal distribution of signals from three channels of the primary system summed over 176 rolls of the spinning rocket. The width of the solar peak corresponds to the detector field of view in the direction normal to the spin axis of the rocket.*

The solar signal is not evident in channel 13 where the signal to background ratio is poorer than in the other channels.

A preliminary solar spectrum, derived from a partial reduction of the flight data, is presented in Figure 3. The statistical uncertainties of these data are small, and in most cases are roughly the size of the points which have been plotted. However, with the exception of the measurements below 3 KeV, the data have *not* been corrected

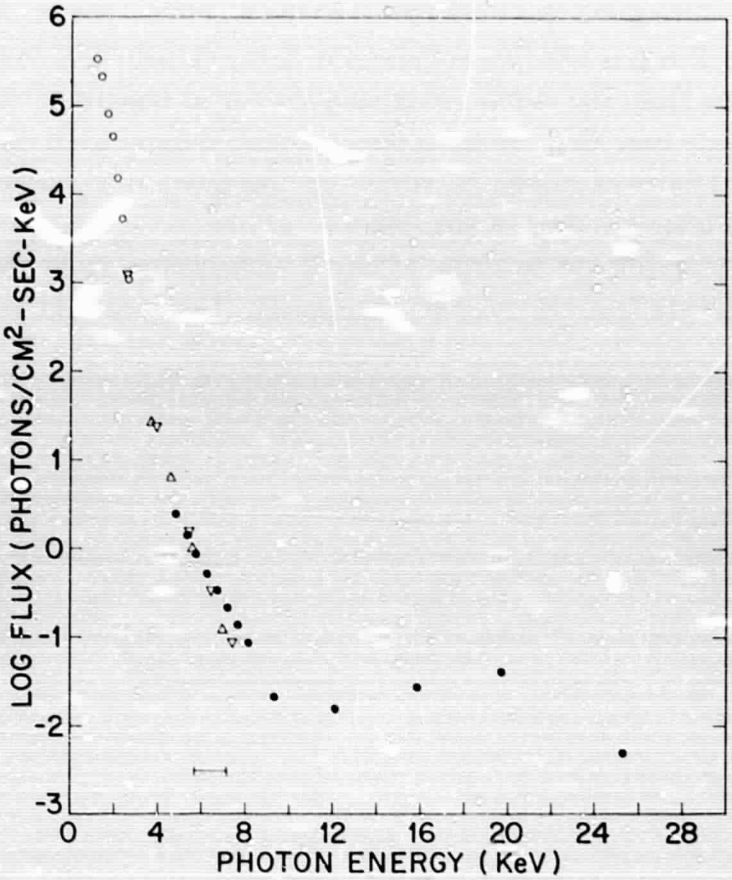


FIG. 3. *Solar X-ray spectrum derived from a preliminary analysis of a portion of the data from four of the five X-ray detection systems flown on April 5, 1967. The data from each system are indicated by different symbols. Those points from the primary system are represented by filled circles. With the exception of the data indicated by the open circles, none of the data have been corrected for system dead-time. It is anticipated that the properly corrected data will not exhibit a pronounced minimum in the spectrum in the 8–14 KeV interval. The horizontal bar indicates the energy resolution (full width at half maximum) of the primary system at 6·4 KeV.*

for the dead-time of the pulse-amplitude measuring systems. These corrections are in general less than 20%, but they may significantly alter the appearance of the spectrum at the higher energies. We anticipate that the apparent minimum in the spectrum in the 8–14 KeV interval will disappear or become less pronounced when the corrections for dead-time are properly taken into account.

## 3. The Interpretation

Figure 4 is a reproduction of a Sacramento Peak Observatory Hα filtergram taken approximately 9½ hours prior to the time of the flight. At the time of the flight there was a complex of old active regions on the Sun in the Northern hemisphere. There were also four active regions in the Southern hemisphere, two of which produced the only flares within 12 hours of our flight. The two extremely active regions that had crossed the disk during the two weeks prior to the flight had passed the Western limb two days earlier. It is possible that some of the X-ray emission recorded by the rocket instruments came from the corona overlying these two regions.

It seems unlikely that 'flare' X-rays contributed to the spectrum of Figure 3. There were no reported flares or sub-flares within the time interval of 3 hours prior to flight time to 7 hours after the time of the flight.

While it is inappropriate to draw extensive conclusions from these preliminary results the following features may be mentioned. The measurements of the solar

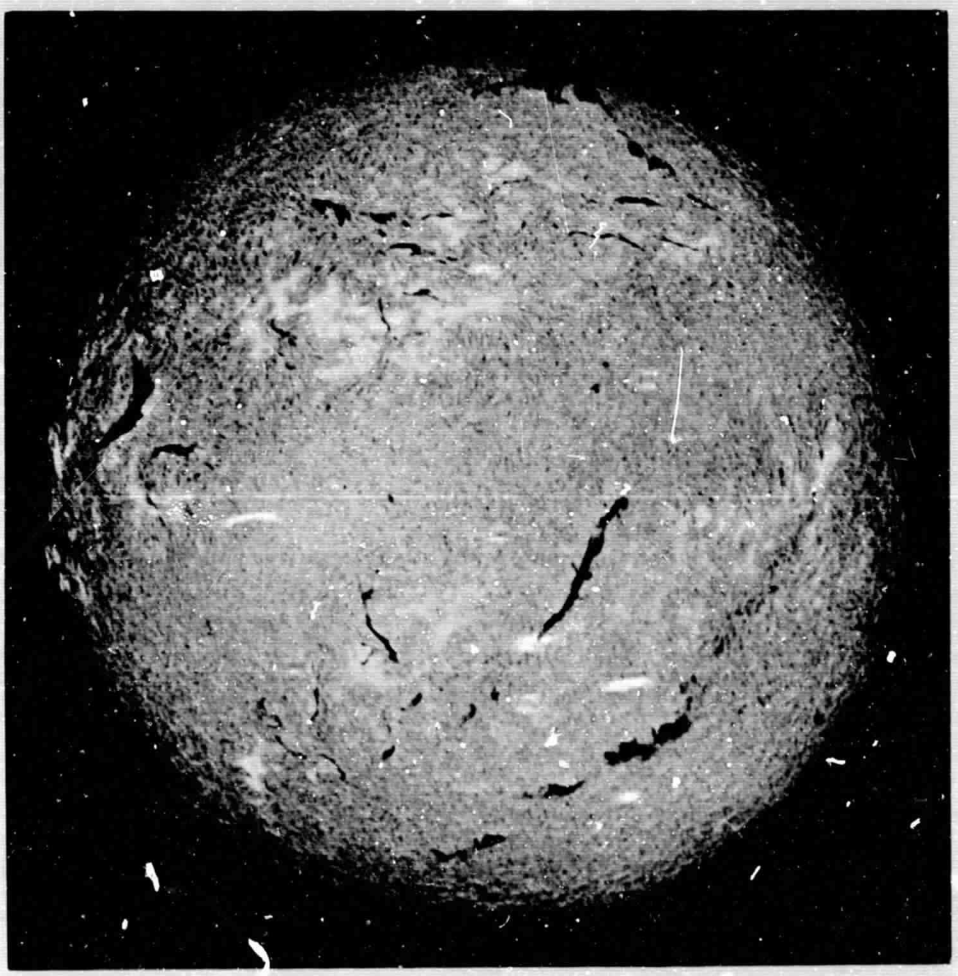

FIG. 4. *Hα filtergram of the Sun taken at 1448 UT on April 4, 1967. (Courtesy of Sacramento Peak Observatory.)*

spectrum at energies below 4 KeV are consistent with those of other workers (Bowles *et al.*, 1967). The observed X-ray intensity lies between that reported by Chodil *et al.* (1965) and that of Underwood given by Bowles *et al.* (1967). Fritz *et al.* (1967) have shown that the X-ray spectrum at energies below 6 KeV is dominated by emission lines.

The slope of the X-ray spectrum above 4 KeV in energy is markedly less steep than at the lower energies. A second change in the nature of the solar X-ray spectrum appears to occur in the 8–12 KeV interval where the spectrum becomes approximately flat, extending to the upper limit of the most reliable data at 22 KeV. The flux which we observed around 15 KeV is almost two decades higher than the upper limit given by Peterson *et al.* (1966) for February 18, 1966 and about five decades below that reported by Chubb *et al.* (1966) from their pioneering observations made in 1959. However, our data appear to be consistent with the measurements reported by Peterson (1967) for the 7·7–12·5 KeV and 12–22 KeV channels of his OSO-3 instrument.

We believe that the extension of the solar X-ray spectrum above approximately 6 KeV is strongly indicative of non-thermal processes taking place in the active regions on the Sun which were quiescent at the time of our flight. Indeed, the relatively flat spectrum extending to high energies beyond 12 KeV may be bremsstrahlung from relativistic electrons either trapped or continually produced within the centres of activity. Further analysis of these data and additional measurements of the kind made during this flight show promise for helping to understand the physics of solar active regions.

**Note added in proof:** It has not yet been possible to reconcile the solar data of the three large-area systems for photon energies greater than 8 KeV. Therefore we consider it advisable to treat with caution the data above 8 KeV from this experiment until such time as these particular measurements are better understood or until independent confirmation of a flat solar X-ray spectrum in the 8-22 KeV interval is obtained.

## References

Bowles, J. A., Culhane, J. L., Sanford, P. W., Shaw, M. L., Cooke, B. A. (1967) *Planet. Space Sci.*, **15**, 931.

Chodil, G., Jopson, R. C., Mark, Hans Seward, F. D., Swift, C. D. (1965) *Phys. Rev. Lett.*, **15**, 605.

Chubb, T. A., Kreplin, R. W., Friedman, H. (1966) *J. geophys. Res.*, **71**, 3611.

Fritz, G., Kreplin, R. W., Meekins, J. F., Unzicker, A. E., Friedman, H. (1967) *Astrophys. J.*, **148**, L133.

Giacconi, R., Reidy, W. P., Zehnpfennig, T., Lindsay, J. C., Muney, W. S. (1965) *Astrophys. J.*, **142**, 1274.

Mathieson, E., Sanford, P. W. (1963) in *Proc. Int'l. Symp. on Nuclear Elec.*, p. 65.

Peterson, L. E. (1967) Paper presented at the XIII General Assembly of the IAU, Prague, August 23, 1967.

Peterson, L.E., Schwartz, D.A., Pelling, R.M., McKenzie, D. (1966) *J. geophys. Res.*, **71**, 5778.
Pounds, K.A., Russell, P.C. (1966) in *Space Research*, VI, p. 38.
Reed, R.D., Bakke, J.C., Reagan, J.B., Acton, L.W. (1968) *IEEE Trans. on Nuclear Sci.*, **NS-16** (in press).
Underwood, J.H., Muney, W.S. (1967) *Solar Phys.*, **1**, 129.
Zhitnik, I.A., Krutov, V.V., Malyavkin, L.P., Mandel'shtam, S.L., Cheremukhin, G.S. (1967) *Kosm. Issled.*, Akad. Nauk SSSR (Moscow), **5**, 276.

END

DATE

FILMED

NOV 18 1969

# A UNIQUE ROCKET-BORNE DATA HANDLING SYSTEM FOR SOLAR X-RAY STUDIES

R. D. Reed, J. C. Bakke, J. B. Reagan and L. W. Acton

Lockheed Palo Alto Research Laboratory
Lockheed Missiles & Space Company
Palo Alto, California

## Summary

A high-speed, high-resolution spectrometer system has been designed for the detection and analysis of low-energy x-rays from a spinning rocket. The system enjoyed a highly successful flight in the spring of 1967 and another flight is currently scheduled for the fall of 1967.

The system was comprised of four large-area beryllium-window proportional counters, an analog pulse-height-to-time converter, a digital data assembler and a complete PCM multiplexer.

The system was capable of analyzing x-ray events at average input rates in excess of 50,000 events per second. The pulse-height-to-time converter, in conjunction with a portion of the digital data assembler, formed a 64-channel pulse-height analyzer and provided an energy resolution of 0.5 keV per channel over the 3-30 keV energy range of the detectors.

The data assembler, using a non-linear, lump digital decoding technique, compiled and stored a complete spectrum on board the rocket. Channel address accumulators were completely buffered so that while one spectrum was being time multiplexed to telemetry, another was being accumulated. This technique gives rise to very short dead-time periods and enabled the detector and pulse-height converter to operate in random-access fashion at high input rates.

The PCM multiplexer portion of the system time multiplexed all of the spectral information, along with absolute rate data, and applicable timing and I.D. information into a serial Non-Return-to-Zero-Level (NRZL) formatted binary output with sufficient drive to directly modulate an FM transmitter. The multiplexer operated from a single, stable 20 kHz oscillator. The timing was such that a complete spectrum, along with rate and timing data, was transmitted each 4.75 milliseconds. A complete frame of 20 spectra, rate and timing signals and all necessary I.D.'s were sent every 0.1 second.

An economical demultiplexer was designed and built for the processing of pre-flight calibration data and for field checkout. This unit accepted the serial wavetrain from the flight instrument and completely demultiplexed it so that the data could be coupled to a standard laboratory pulse-height analyzer for storage, visual display and complete print-out capability. The demultiplexer processed all of the data in a completely digital fashion from the same 20 kHz clock that was in the flight package, so that no D-A and A-D conversion errors were introduced by the demultiplexer or laboratory PHA.

## Introduction

In an effort to gain data that would lead to a better understanding of the physical nature of active regions of the sun, a rocket-borne instrument package was designed and built at the Lockheed Palo Alto Research Laboratory to study the x-ray emissions from these regions in their quiescent state. The experiment was accomplished by launching the instrument package on a spin-stabilized Aerobee rocket from White Sands Missile Range, New Mexico, at 0015 UT on 5 April 1967. The experimental objective of this flight was the measurement of solar x-ray emissions in the 1-30 keV region.

The primary spectrometer of this package, which made spectral measurements of x-rays in the 3-30 keV region, will be described in this paper. The spectrometer consisted of four large-area gas proportional counters whose outputs were parallel coupled to a Pulse-Height Analyzer (PHA) and a Digital Data Assembler and Multiplexer (DDA&M). The PHA and DDA&M were designed as an integral part of the instrument in an effort to realize the full capability of the radiation detectors while maintaining compatibility with the rocket telemetry system. The overall block diagram of the spectrometer is shown in Figure 1.